HHS Public Access

Author manuscript

Biochem Pharmacol. Author manuscript; available in PMC 2017 February 01.

Published in final edited form as:

Biochem Pharmacol. 2016 February 1; 101: 54–70. doi:10.1016/j.bcp.2015.11.026.

Pioglitazone, a PPARγ agonist, attenuates PDGF-induced vascular smooth muscle cell proliferation through AMPK-dependent and AMPK-independent inhibition of mTOR/p70S6K and ERK signaling

Islam Osman[a,b] and **Lakshman Segar**[a,b,c,d,*]

[a]Center for Pharmacy and Experimental Therapeutics, University of Georgia College of Pharmacy, Augusta, Georgia, USA

[b]Charlie Norwood VA Medical Center, Augusta, Georgia, USA

[c]Vascular Biology Center, Department of Pharmacology and Toxicology, Georgia Regents University, Augusta, Georgia, USA

[d]Department of Medicine, Pennsylvania State University College of Medicine, Hershey, Pennsylvania, USA

Abstract

Pioglitazone (PIO), a PPARγ agonist that improves glycemic control in type 2 diabetes through its insulin-sensitizing action, has been shown to exhibit beneficial effects in the vessel wall. For instance, it inhibits vascular smooth muscle cell (VSMC) proliferation, a major event in atherosclerosis and restenosis after angioplasty. Although PPARγ-dependent and PPARγ-independent mechanisms have been attributed to its vasoprotective effects, the signaling events associated with PIO action in VSMCs are not fully understood. To date, the likely intermediary role of AMP-activated protein kinase (AMPK) toward PIO inhibition of VSMC proliferation has not been examined. Using human aortic VSMCs, the present study demonstrates that PIO activates AMPK in a sustained manner thereby contributing in part to inhibition of key proliferative signaling events. In particular, PIO at 30 μM concentration activates AMPK to induce raptor phosphorylation, which diminishes PDGF-induced mTOR activity as evidenced by decreased phosphorylation of p70S6K, 4E-BP1, and S6 and increased accumulation of $p27^{kip1}$, a cell cycle inhibitor. In addition, PIO inhibits the basal phosphorylation of ERK in VSMCs. Downregulation of endogenous AMPK by target-specific siRNA reveals an AMPK-independent effect for PIO inhibition of ERK, which contributes in part to diminutions in cyclin D1 expression and Rb phosphorylation and the suppression of VSMC proliferation. Furthermore, AMPK-dependent inhibition of mTOR/p70S6K and AMPK-independent inhibition of ERK signaling occur

*Corresponding author at: Lakshman Segar, Center for Pharmacy and Experimental Therapeutics, University of Georgia College of Pharmacy, 1120 15th Street, HM-1200, Georgia Regents University Campus, Augusta, Georgia, USA 30912-2450. Tel: +1 706 721 6491; fax: +1 706 721 3994, lsegar@gru.edu.

regardless of PPARγ expression/activation in VSMCs as evidenced by gene silencing and pharmacological inhibition of PPARγ. Strategies that utilize nanoparticle-mediated PIO delivery at the lesion site may limit restenosis after angioplasty without inducing PPARγ-mediated systemic adverse effects.

Graphical Abstract

PIO inhibits PDGF-induced vascular smooth muscle cell proliferation *via* AMPK-dependent inhibition of mTOR/p70S6 kinase and AMPK-independent inhibition of ERK1/2 signaling

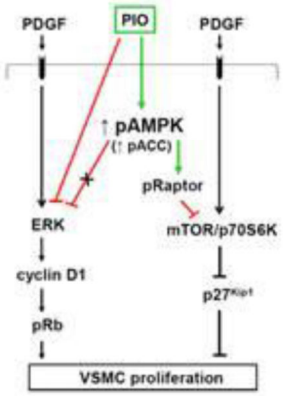

Keywords

vascular smooth muscle cells; pioglitazone; AMPK; p70S6K; ERK

1. Introduction

Vascular smooth muscle cell (VSMC) proliferation is a major event in the development of atherosclerosis and restenosis after angioplasty [1, 2]. Thiazolidinediones (TZDs) have been shown to exhibit beneficial effects in the vessel wall [3-5] beyond their insulin-sensitizing action that improves glycemic control in patients with type 2 diabetes [6]. Yet, TZD treatment is associated with several adverse effects, including weight gain, fluid retention, and congestive heart failure, thus raising concerns about their cardiovascular safety [7]. These unfavorable effects are attributed in part to activation of peroxisome proliferator activated receptor-γ (PPARγ). For instance, TZD activation of PPARγ in the renal collecting duct stimulates epithelial sodium channel transcription to promote sodium absorption and fluid accumulation [8, 9]. Notably, PPARγ is also expressed in VSMCs but to a modest extent [10-13], compared with its abundant expression level in adipose tissue [10]. Although previous studies have reported PPARγ-dependent and PPARγ-independent mechanisms for TZD inhibition of VSMC proliferation [14-20], the signaling events associated with TZD action in VSMCs are not fully understood.

TZDs such as rosiglitazone (ROSI) and pioglitazone (PIO) are currently in clinical use but are prescribed with caution due to the risk of congestive heart failure [21, 22]. Troglitazone (TRO) has been withdrawn from market due to hepatotoxicity [21]. While commonly being

referred to as PPARγ agonists, PPARγ binding affinity for ROSI is several fold greater than PIO or TRO [23]. Despite their differences in PPARγ binding affinities, all three TZDs exhibit comparable inhibitory effects on VSMC proliferation [11, 17] by affecting cell cycle regulatory events critical for G1→S progression [16, 17]. The key proliferative signaling components in VSMCs include MEK1/ERK and mTOR/p70S6K that undergo activation upon challenge with mitogens including platelet-derived growth factor (PDGF) or angiotensin II [24-26]. In this regard, TZDs have been shown to inhibit mitogen-induced activation of ERK signaling in VSMCs [13, 15, 18, 27]. Importantly, TZD treatment results in the activation of AMP-activated protein kinase (AMPK) in insulin-responsive tissues/cells [28-31] and endothelial cells [32], but such effect has not yet been reported in VSMCs. AMPK activation in VSMCs (e.g., by AICAR or adipokines) is associated with inhibition of ERK activation [25, 33, 34]. In addition, AMPK activation leads to inhibition of mTOR/p70S6K signaling in different tissues/cell types [35, 36], including VSMCs [37]. Notably, AMPK activation in nonvascular cells promotes raptor phosphorylation to inhibit the activity of mTOR [38]. Hence, it is critically important to examine the likely intermediary role of AMPK toward TZD suppression of key proliferative signaling events in VSMCs.

In skeletal muscle cells and hepatocytes, TZD activation of AMPK has been shown to involve mitochondrial membrane depolarization, a decrease in cellular ATP level, an increase in AMP that binds to AMPKγ subunit to facilitate allosteric activation, and enhanced phosphorylation of Thr^{172} residue in AMPKα unit by LKB1, an upstream kinase for AMPK [28, 30, 39]. In addition, AMPK activation leads to phosphorylation and inactivation of acetyl CoA carboxylase (ACC), a key downstream target of AMPK [39]. Nevertheless, it remains unknown as to whether TZD affects cellular energy state to promote AMPK activation in VSMCs.

The objectives of the present study using human aortic VSMCs are to determine: i) the extent to which PIO regulates the phosphorylation AMPKα^{Thr172} and its downstream target, ACC; ii) PIO regulation of cellular energy state including mitochondrial membrane potential (by TMRM fluorescence analysis) and AMP/ATP ratio (by LC-MS/MS MRM analysis); iii) the role of LKB1 as a likely upstream kinase; iv) the extent to which PIO activation of AMPK regulates PDGF-induced key proliferative signaling events including mTOR/p70S6K and ERK; and v) whether PIO regulation of key proliferative signaling is dependent on PPARγ expression.

2. Materials and methods

2.1. Materials

Pioglitazone, rosiglitazone, and GW-9622 were purchased from Cayman Chemical Company (Ann Arbor, MI). Recombinant human PDGF-BB was purchased from R&D Systems (Minneapolis, MN). The primary antibodies for phospho-AMPKα^{Thr172} (2535), pan-AMPKα (2532), AMPKα1 (2795), AMPKα2 (2757), phospho-ACC^{Ser79} (11818), ACC (3676), phospho-LKB1^{Ser428} (3482), LKB1 (3047), phospho-44/42 MAPK (ERK1/2; 4695), 44/42 MAPK (ERK1/2; 9102), phospho-Akt^{Thr308} (2965), Akt (4691), phospho-GSK3β^{Ser9} (9323), GSK3β (12456), phospho-p70S6K^{Thr389} (9234), p70S6K (2708), phsopho-4E-BP1^{Ser65} (9451), 4E-BP1 (9644), phospho-S6 ribosomal protein$^{Ser235/236}$ (4857), S6

ribosomal protein (2217), phospho-Raptor^{Ser792} (2083), Raptor (2280), PPARγ (2435), p27^{Kip1} (3686), cyclin D1 (2922), phospho-Rb^{Ser795} (9301), phospho-p53^{Ser15} (9286), p53 (2524), p21^{Cip1} (2947), CD36 (14347), and β-actin (8457) were purchased from Cell Signaling Technology (Danvers, MA). The primary antibody for SM α-actin (ab5694) was purchased from Abcam (Cambridge, MA). The primary antibody for calponin (C2687) was purchased from Sigma Chemical (St. Louis, MO). LKB1, AMPKα1, AMPKα2, PPARγ silencer select siRNAs and scrambled siRNA were purchased from Life Technologies (Carlsbad, CA). Adenosine 5'-triphosphate disodium (ATP), adenosine 5'-diphosphate monosodium (ADP), and adenosine 5'-monophosphate disodium (AMP) were purchased from EMD Millipore Chemicals (Billerica, MA). All other chemicals were from Fisher Scientific (Fair Lawn, NJ) or Sigma Chemical (St. Louis, MO).

2.2. Cell culture and treatments

Human aortic VSMCs, vascular cell basal medium and smooth muscle growth supplement (SMGS) were purchased from ATCC (Manassas, VA). SMGS constituents and their final concentrations after addition to vascular cell basal medium were as follows: 5% FBS (vol/vol), 5 ng/ml human basic fibroblast growth factor, 5 ng/ml human epidermal growth factor, 5 μg/ml insulin, 50 μg/mL ascorbic acid, 10 mM L-Glutamine. VSMCs (passages 3-5) were incubated in vascular cell basal medium containing SMGS (complete medium) and 5.5 mM D-glucose along with antibiotic/antimycotic solution in a humidified atmosphere of 95% air and 5% CO_2 at 37°C. After the attainment of confluence (~6-7 days), VSMCs were trypsinized, centrifuged, and seeded onto petri dishes or multiwell plates. Subconfluent VSMCs were maintained under SMGS (serum)-deprived conditions for 48 hours to achieve quiescence, and then subjected to treatments as described in the legends to the respective figures. DMSO (0.1%) was used as the vehicle control for PIO or ROSI treatment.

2.3. Cell counts

Subconfluent VSMCs were serum-deprived for 48 hr and then pretreated with PIO (3, 10 or 30 μM, 30 min) or vehicle control followed by exposure to PDGF (30 ng/ml, 96 hr). We replaced the medium with fresh serum-free medium containing the indicated concentrations of PIO and/or PDGF every 48 hr. VSMCs were then trypsinized and the changes in cell number were determined using Countess Counter (Life Technologies), as described [40].

2.4. DNA synthesis assay

Serum-deprived VSMCs were treated with PIO (30 μM) or vehicle control for 24 hr and then exposed to PDGF (30 ng/ml) for another 24 hr. DNA synthesis was measured using click iT® EdU microplate assay according to the manufacturer's instructions (Life technologies). In brief, VSMCs were incubated with 5-ethynyl-2'-deoxyuridine (EdU; a nucleoside analog) during the last 18 hr of respective treatments. Subsequently, cells were exposed to the supplied fixative reagent followed by labeling of EdU with green-fluorescent Oregon Green® azide. Signal amplification was then achieved by incubation with HRP-conjugated anti-Oregon Green® antibody followed by reaction with Amplex® UltraRed substrate that produces a brightly red fluorescent product (excitation/emission: 568/585 nm).

2.5. Immunoblot analysis

VSMC lysates (20 μg protein per lane) were subjected to electrophoresis using precast 4-12% NuPage mini-gels (Life Technologies). The resolved proteins were then transferred to PVDF membranes (EMD Millipore). Subsequently, the membranes were blocked in 5% nonfat milk and probed with the respective primary antibodies. The immunoreactivity was detected using HRP-conjugated horse anti-mouse secondary antibody (7076; Cell Signaling) or goat anti-rabbit secondary antibody (7074; Cell Signaling) followed by enhanced chemiluminescence (ECL; Thermo Scientific, Wilmington, DE). Immunoblots for ECL detection of a given protein target and its phosphorylated form were run in parallel. β-actin was used as an internal control. The displayed β-actin in the respective figures is representative of β-actin immunoreactivity for all blots. The protein bands shown in respective figures represent the results obtained from at least three separate independent experiments. The protein bands were quantified using Image J.

2.6. Assessment of mitochondrial membrane potential

Mitochondrial membrane potential ($\Delta\psi$) was determined using a MitoPT TMRM assay kit according to manufacturer's instructions (ImmunoChemistry Technologies, Bloomington, MN). Briefly, serum-deprived VSMCs were exposed to PIO (30 μM) for 1 or 3 hr, or vehicle control. Subsequently, VSMCs were stained with tetramethylrhodamine methyl ester (TMRM, 200 nM, 20 min at 37°C in the dark), washed with 1 ml wash buffer, and then visualized by fluorescence microscopy (Zeiss, Thornwood, NY). In intact cells, the cationic nature of TMRM allows it to accumulate within the inner membrane region of polarized mitochondria, resulting in a marked increase in TMRM-associated orange fluorescence. When mitochondrial membrane depolarizes, TMRM gets dispersed throughout the cytosol at a concentration that yields minimal fluorescence upon excitation. Thus, mitochondrial membrane potential was assessed by examination of TMRM-associated orange fluorescence (Excitation/Emission: 548 nm/573 nm). Carbonylcyanide m-chlorophenylhydrazone (CCCP, 50 μM, 1 hr) a generic mitochondrial membrane depolarizer, was used as a positive control.

2.7. Quantification of adenine nucleotides (ATP, ADP, and AMP) using LC-MS/MS MRM

Quantification of adenine nucleotides in VSMCs was done as previously described [41]. Briefly, serum-deprived VSMCs were exposed to PIO (30 μM, 3hr) or vehicle control. VSMCs were collected in ice-cold PBS, lysed in ice-cold 5% perchloric acid, and then centrifuged at 10,000 × g for 5 min at 4°C to remove the acid-insoluble material. Perchloric acid in the collected supernatant was extracted by three washes with 10% excess volume of a 1:1 mixture of tri-n-octylamine and 1,1,2-trichlorotrifluroethane. Adenine nucleotides in the aqueous phase were analyzed using liquid chromatography/tandem mass spectrometry (LC-MS/MS) with multiple reaction monitoring (MRM) on a 4000 QTRAP LC/MS/MS system (Applied Biosystems, Carlsbad, CA). The samples and standards were run on a Amide XBridge HPLC column (Cat # 186004860; 3.5 μM particle size; 2.1 mm inner diameter × 100 mm length, Waters, Milford, MA) using buffer A (20 mM ammonium hydroxide and 20 mM ammonium acetate in 5% acetonitrile, pH 9.0) and buffer B (100% acetonitrile) at a flow rate of 0.3 ml/min for 10 min. The mobile phase consists of isocratic elusion with 20% buffer B. The concentrations of AMP, ADP and ATP were calculated

from standard curves of a serial dilution of a standard consisting of known concentrations of AMP, ADP and ATP that were run in parallel with the samples in the same session.

2.8. Nucleofection of VSMCs with target-specific siRNAs

Subconfluent VSMCs were transfected with 500 pmoles of target-specific Silencer® Select Pre-Designed siRNA (Life technologies, Carlsbad, CA) using the Amaxa nucleofector-II device U-025 program (Lonza, Germany). The scrambled siRNA- and target-specific siRNA-transfected VSMCs were incubated in complete medium for 48 hr. Subsequently, VSMCs were serum-deprived for 24 hr and then subjected to treatments as described in the legends to the respective figures.

2.9. Nascent protein synthesis assay

Serum-deprived VSMCs were exposed to PIO (30 μM) or vehicle control for 24 hr in the absence or presence of PDGF (30 ng/ml). Nascent protein synthesis was determined using click-iT® Plus OPP Alexa Fluor® 488 protein synthesis assay kit according to the manufacturers' instructions (Life Technologies). Briefly, VSMCs were incubated with 20 μM Click-iT® OPP working solution for 30 min, fixed with 4% paraformaldehyde in PBS, permeabilized with 0.5% Triton X-100 in PBS. VSMCs were then incubated with Click-iT® Plus OPP reaction cocktail for 30 min at room temperature, protected from light, and incubated with NuclearMask™ Blue Stain to label nuclei. Nascent protein synthesis was assessed by determination of signal intensity in the green fluorescent channel as determined by confocal microscopy (Zeiss, Thornwood, NY).

2.10. RNA extraction, cDNA synthesis and real-time quantitative RT-PCR (qRT-PCR)

RNA extraction, cDNA synthesis and qRT-PCR were performed as previously described [40]. Briefly, total RNA was extracted from VSMCs by RNeasy mini-kit (Qiagen, Valencia, CA) and then treated with RNase-free DNase I (Qiagen) to remove contamination due to genomic DNA. RNA quantification and purity assessment were performed spectroscopically using NanoDrop 2000 spectrophotometer (Thermo Scientific). 500 ng of total RNA was reverse transcribed to cDNA by Superscript First Strand RT-PCR system (Life Technologies) using oligo(dT) primers. qRT-PCR analysis was performed using Applied Biosystems 7900HT Fast Real-Time PCR system and QuantiTect SYBR Green PCR kit (Qiagen). Relative mRNA expression values were determined by the comparative threshold cycle (C_T) method. C_T values were normalized with internal control gene β2 microglobulin (β2M). Cyclin D1 primer sequences were as follows: Forward primer (5'-TGTCCTACTACCGCCTCACA-3') and reverse primer (5'-TCCTCCTCTTCCTCCTCCTC-3'). β2M primer sequences were as follows: Forward primer (5'-TGGTCTTTCTGGTGCTTGTCT-3') and reverse primer (5'-TATGTTCGGCTTCCCATTCT-3').

2.11. Nuclear and cytoplasmic protein extraction

Nuclear and cytoplasmic protein fractions were obtained using a nuclear and cytoplasmic extraction kit according to manufacturer's instructions (Thermo Scientific). Briefly, serum-deprived VSMCs were exposed to PIO (30 μM) or vehicle control for 48 hr. Cells were

harvested with trypsin-EDTA and then centrifuged at 500 × g for 5 min. The cell pellet was washed with ice-cold PBS. Subsequently, ice-cold cytoplasmic extraction reagents (CER I and CER II) were mixed with protease/phosphatase inhibitor cocktail (Thermo Scientific) and added to the cell pellet to cause cell membrane disruption and the release of cytoplasmic contents. After recovering the nuclear pellet from the cytoplasmic extract by centrifugation (16,000 × g for 5 min), the nuclear proteins were extracted with the nuclear extraction reagent (NER) plus protease/phosphatase inhibitor cocktail.

2.12. Statistical analysis

Results are expressed as the means ± SEM of at least three separate experiments. Statistical analyses of the data were performed using one-way analysis of variance (ANOVA) followed by Bonferroni t-test for data involving more than two groups, or unpaired two-tailed t-test for data involving two groups only. Values of $p < 0.05$ were considered statistically significant.

3. Results

3.1. PIO inhibits PDGF-induced VSMC proliferation

Previous studies have shown that TZDs suppress mitogen-induced VSMC proliferation [14-17, 42], by affecting the cell cycle regulatory events critical for G1→S progression [16, 17]. In the present study, we examined the effects of PIO on PDGF-induced VSMC proliferation, DNA synthesis, and the associated changes in cell cycle proteins. Prior to treatments, VSMCs were maintained under serum-deprived conditions to promote transition to a contractile phenotype. As shown in Fig. 1A, serum deprivation led to an increase in the expression of SM α-actin and calponin by ~7 ± 0.3- and 6 ± 0.2-fold, respectively. Fig. 1B shows that PIO treatment, by itself, did not affect basal VSMC proliferation at 3 to 30 μM concentrations. However, it diminished PDGF-induced VSMC proliferation by 18 ± 10% ($p = 0.9$), 42 ± 14% ($p = 0.4$), and 84 ± 6% ($p < 0.05$) at 3, 10, and 30 μM concentrations, respectively. In addition, PIO at 30 μM concentration did not affect basal DNA synthesis but significantly decreased PDGF-induced DNA synthesis by 96 ± 3% ($p < 0.05$) (Fig. 1C). Together, PIO treatment shows a trend toward a decrease in PDGF-induced VSMC proliferation at 10 μM concentration with a more pronounced inhibition at 30 μM concentration.

Furthermore, PIO treatment led to significant inhibition of PDGF-induced increase in cyclin D1 expression by 32 ± 10% ($p < 0.05$) and 97 ± 8% ($p < 0.05$) at 10 and 30 μM concentrations, respectively (Fig. 1D). It also inhibited PDGF-induced increase in Rb phosphorylation by 42 ± 4% ($p < 0.05$) and 93 ± 11% ($p < 0.05$) at 10 and 30 μM concentrations, respectively. Importantly, PIO, by itself, enhanced the accumulation of $p27^{Kip1}$ (a cell cycle inhibitor) [43] by 35 ± 7% ($p < 0.05$) and 43 ± 9% ($p < 0.05$) at 10 μM and 30 μM concentrations, respectively. In addition, PIO prevented PDGF-induced degradation of $p27^{Kip1}$ by ~83 ± 13%. At all three concentrations used in this study, PIO did not affect the viability of VSMCs as determined by trypan blue exclusion test.

Since TRO and ROSI have previously been shown to attenuate mitogen-induced $p21^{Cip1}$ expression in VSMCs [16], we examined the effects of PIO on $p21^{Cip1}$ expression in PDGF-exposed VSMCs. As shown in Fig. 1E, PIO at 30 μM concentration significantly diminished the basal expression of $p21^{Cip1}$ by 47 ± 4 %. In addition, PIO treatment led to a significant decrease in PDGF-induced $p21^{Cip1}$ expression, compared with PDGF alone. Since p53 activation and its accumulation have been shown to inhibit VSMC proliferation [44], we also examined the effects of PIO on p53 in VSMCs. Neither PIO treatment nor PDGF stimulation affected the phosphorylation or expression level of p53 in VSMCs.

Thus, PIO inhibition of PDGF-induced VSMC proliferation was associated with accumulation of $p27^{Kip1}$ and diminutions in $p21^{Cip1}$ expression, cyclin D1 expression, and Rb phosphorylation.

3.2. PIO enhances the phosphorylation of AMPK and ACC as a function of concentration and time in VSMCs

TZD activation of AMPK has been demonstrated in insulin-responsive tissues/cells (e.g., skeletal muscle, adipose tissue, and liver) [28-31] and endothelial cells [32] but not in VSMCs. Since AMPK activation has been shown to regulate key proliferative signaling events such as MEK1/ERK [25, 33, 34] and mTOR/p70S6K [37] in VSMCs, we examined the likely regulatory effects of TZDs on AMPK and its downstream target, ACC. As shown in Fig. 2A, exposure of VSMCs to PIO at 3, 10, and 30 μM concentrations led to a progressive increase in the phosphorylation of $AMPK^{Thr172}$ by ~1.9 ± 0.2-, 2.3 ± 0.1-, and 3.6 ± 0.1-fold, respectively. This increase in $AMPK^{Thr172}$ phosphorylation by PIO was accompanied by significant increases in ACC phosphorylation. In addition, PIO treatment at 30 μM concentration resulted in a time-dependent increase in $AMPK^{Thr172}$ phosphorylation between 3 hr and 48 hr (Fig. 2B). Furthermore, PIO induced a sustained increase in ACC phosphorylation between 1 hr and 48 hr. Under the same treatment conditions, PIO did not induce any changes in the phosphorylation of LKB1, an upstream kinase for AMPK [39]. To determine whether a different TZD derivative could activate AMPK in VSMCs, select studies examined the effects of rosiglitazone (ROSI) *versus* PIO. As shown in Fig. 2C, exposure of VSMCs to ROSI (30 μM) led to an increase in the phosphorylation of $AMPK^{Thr172}$ and ACC at 24 hr, much greater than that observed at 48 hr time point. In parallel, PIO enhanced the phosphorylation of $AMPK^{Thr172}$ and ACC at 24 hr (to an extent similar to ROSI), but induced a further increase in the phosphorylation of $AMPK^{Thr172}$ and ACC at 48 hr time point (unlike ROSI). Thus, PIO activation of AMPK occurred in a more sustained manner compared with rosiglitazone.

3.3. PIO activates AMPK independent of LKB1 in VSMCs

Although PIO did not affect LKB1 phosphorylation (as shown in Fig. 2A-B), we further verified whether LKB1 expression is required for PIO activation of AMPK. This is because previous studies have shown that injury-induced neointima formation is associated with suppression of LKB1 and AMPK activity [45]. As shown in Fig. 3A-B, transfection of VSMCs with target-specific siRNA led to downregulation of LKB1 by ~86 ± 4%. In addition, LKB1 downregulation did not result in significant changes in basal or PIO-induced phosphorylation of AMPK and ACC.

3.4. PIO does not affect mitochondrial membrane potential or AMP/ATP ratio in VSMCs

TZD activation of AMPK in skeletal muscle cells is mediated by a reduction in mitochondrial membrane potential and/or an increase in AMP/ATP ratio [28, 30, 46]. Hence, we also examined whether the observed activation of AMPK by PIO is due to changes in cellular energy state. As shown in Fig. 4A, exposure of VSMCs to 30 μM PIO did not affect mitochondrial membrane potential at 1 hr or 3 hr time points. The effect of CCCP (50 μM, 1 hr), a generic mitochondrial membrane depolarizer, was examined in parallel and thus served as a positive control. In addition, the effects of PIO (30 μM) on adenine nucleotides levels (AMP, ADP and ATP) were examined at the 3 hr time point, using LC-MS/MS MRM analysis. PIO treatment resulted in a marginal but insignificant increase in AMP/ATP ratio (Fig. 4B). Collectively, these data suggest that PIO-induced AMPK activation in VSMCs occurs independent of changes in mitochondrial membrane potential or AMP/ATP ratio.

3.5. PIO inhibits basal ERK phosphorylation, and PDGF-induced mTOR/p70S6K signaling and protein synthesis

Previously, we and several other investigators have shown that mitogen-induced VSMC proliferation is mediated by activation of different signaling pathways, including MEK/ERK, PI3K/Akt, and mTOR/p70S6K [24-26]. In the present study, we examined whether PIO suppression of PDGF-induced VSMC proliferation occurs through inhibition of these key signaling components. As shown in Fig. 5A, pretreatment with PIO alone led to a significant diminution in basal ERK1/2 phosphorylation by ~80%. Exposure of control and PIO-treated VSMCs to PDGF resulted in a significant increase in ERK1/2 phosphorylation by ~4.2-fold and ~9.3-fold, respectively. Thus, PIO treatment reduced basal ERK1/2 phosphorylation but not PDGF-induced ERK phosphorylation. Fig. 5B shows that PIO did not affect PDGF-induced phosphorylation of Akt (Thr^{308}) or its downstream effector GSK-3β (Ser^{9}). With regard to mTOR/p70S6K signaling, PIO diminished both basal and PDGF-induced phosphorylation of p70S6K^{Thr389}, and its downstream effectors, 4E-BP1 (Ser^{65}) and S6 ribosomal protein (S6, $Ser^{235/236}$) (Fig. 5C). Since mTOR activation is associated with cell growth *via* enhanced protein synthesis [47], we also studied the effects of PIO on PDGF-induced protein synthesis. As shown in Fig. 5D-E, pretreatment with PIO (30 μM, 30 min) inhibited PDGF (30 ng/ml, 24 hr)-induced protein synthesis by ~63 ± 15 %. Together, these data suggest that PIO attenuates VSMC proliferation by inhibiting ERK and p70S6K signaling pathways.

3.6. AMPK mediates PIO-induced inhibition of S6 phosphorylation and accumulation of $p27^{kip1}$

Recently, regulatory associated protein of mTOR (Raptor), a scaffolding protein that provides a bridge between mTOR and its downstream targets, has been identified as a direct substrate of AMPK that undergoes phosphorylation (Ser^{792}) to facilitate allosteric inhibition of mTOR activity [38, 48]. In conformity with these reports, the present findings reveal that PIO treatment (30 μM) was associated with enhanced raptor phosphorylation (Ser^{792}) in VSMCs, suggesting an intermediary role of AMPK toward inhibition of mTOR/p70S6K signaling (Fig. 6D). Next, we examined whether AMPKα1 or AMPK α2 isoform

contributes to this effect. As shown in Fig. 6A-C, transfection of VSMCs with target-specific siRNA led to downregulation of AMPKα1 and AMPKα2 isoforms by ~75 ± 2% and ~50 ± 6 %, respectively. Downregulation of AMPKα1, but not AMPKα2, markedly inhibited PIO (30 μM, 48 hr)-induced AMPK and ACC phosphorylation, indicating that AMPKα1 mediates PIO-induced AMPK activation (Fig. 6A). Importantly, AMPKα1 downregulation prevented PIO-mediated increase in raptor phosphorylation and the concomitant decrease in PDGF-induced S6 phosphorylation, thus providing direct evidence for the intermediary role of AMPK in PIO-mediated inhibition of mTOR/p70S6K signaling in VSMCs (Fig. 6D). In addition, AMPKα1 downregulation prevented PIO-mediated accumulation of $p27^{kip1}$ (Fig. 6D).

Since we observed PIO inhibition of ERK1/2 phosphorylation and cyclin D1 expression (sections *3.5* and *3.1*, respectively), the intermediary role of AMPK in these effects was also examined. AMPKα1 downregulation did not alter PIO-mediated inhibitory effects on ERK1/2 phosphorylation or cyclin D1 expression, indicating that these effects were independent of AMPK activation (Fig. 6E). Collectively, these data suggest that PIO inhibits VSMC proliferation by at least two independent mechanisms: activation of AMPK/mTOR/$p27^{kip1}$ and inhibition of ERK signaling pathways.

3.7. PIO downregulates cyclin D1 mRNA in VSMCs

MEK/ERK signaling pathway is the well-characterized pathway controlling the transcription of cyclin D1. Accordingly, we examined if PIO-mediated inhibition of basal ERK1/2 phosphorylation was associated with transcriptional repression of cyclin D1. Quantitative RT-PCR analysis revealed that exposure of serum-deprived VSMCs to PIO (30 μM, 48 hr) resulted in ~65 ± 3% decrease in cyclin D1 mRNA, compared with vehicle control ($p < 0.05$; $n = 3$). These data suggest that PIO inhibition of basal ERK1/2 phosphorylation is likely responsible for the observed transcriptional repression of cyclin D1.

3.8. PIO activates AMPK and inhibits S6 phosphorylation, ERK1/2 phosphorylation and cyclin D1 expression independent of PPARγ

TZDs, including PIO, are potent activators of PPARγ and thus have robust insulin-sensitizing activities. Although PPARγ is abundantly expressed in adipose tissue, it is expressed to a modest extent in several other tissues/cells, including VSMCs [10, 11]. Thus, we examined whether PIO-mediated AMPK activation and the associated changes in signaling components are mediated through the activation of PPARγ. Using differentiated 3T3-L1 cells as a positive control that express both PPARγ1 and PPARγ2, we confirmed previous reports that PPARγ1 protein is expressed in human aortic VSMCs and was localized predominantly in the nuclear fraction (Fig. 7A). Exposure of VSMCs to PIO (30 μM, 48 hr) led to a marked increase in PPARγ expression in the nuclear fraction (Fig. 7A) and in whole cell lysate (Fig. 7B). In mock-transfected VSMCs (using scrambled siRNA), PIO treatment led to a significant increase in the expression of PPARγ (by ~3 ± 0.6-fold) and its target gene [49], CD36 (by ~2 ± 0.5-fold) (Fig. 7B). Importantly, downregulation of PPARγ expression (~87 ± 3%) by target-specific siRNA prevented PIO-induced CD36 expression (Fig. 7B-C). However, it did not alter PIO-mediated AMPK phosphorylation or PIO inhibition of PDGF-induced S6 phosphorylation (Fig. 7D). Moreover, PPARγ

downregulation did not alter PIO-mediated inhibition of basal ERK1/2 phosphorylation or PDGF (30 ng/ml, 48 hr)-induced cyclin D1 expression. To confirm these results, we pretreated VSMCs with GW-9662 (10 μM, 30 min), an inhibitor of PPARγ, before PIO treatment. As shown in Fig. 7E, GW-9662 did not affect any of the aforementioned signaling events in VSMCs.

4. Discussion

The present study demonstrates that the antidiabetic drug, pioglitazone (PIO), activates AMPK in a sustained manner thereby contributing in part to inhibition of key proliferative signaling events in VSMCs (Fig. 8). In particular, PIO at 30 μM concentration activates AMPK to induce raptor phosphorylation, which diminishes PDGF-induced mTOR activity as evidenced by decreased phosphorylation of p70S6K, 4E-BP1, and S6 and increased accumulation of $p27^{kip1}$, a cell cycle inhibitor. In addition, PIO inhibits the basal phosphorylation of ERK in VSMCs. Downregulation of endogenous AMPK by target-specific siRNA reveals an AMPK-independent effect for PIO inhibition of ERK, which contributes in part to diminutions in cyclin D1 expression and Rb phosphorylation and the suppression of VSMC proliferation. Furthermore, AMPK-dependent inhibition of mTOR/p70S6K and AMPK-independent inhibition of ERK signaling occur regardless of PPARγ expression/activation in VSMCs as evidenced by gene silencing and pharmacological inhibition of PPARγ. Strategies that utilize nanoparticle-mediated PIO delivery at the lesion site may limit restenosis after angioplasty without inducing PPARγ-mediated systemic adverse effects [50, 51].

Previous studies demonstrate that AMPK activation suppresses VSMC proliferation [25, 34, 44, 52], whereas genetic and pharmacological strategies to inactivate AMPK restore VSMC proliferative response [25, 34, 44]. Unlike these earlier observations with an AMPK activator (e.g., AICAR) [25, 44, 52], the present findings with a TZD derivative (e.g., PIO) highlight its role in AMPK activation that mediates the suppression of VSMC proliferative signaling in a partial manner. Notably, ectopic expression of dominant-negative AMPK to inhibit AMPK activity [25, 44] prevents AICAR inhibition of serum-induced VSMC proliferation and the associated phosphorylation of Rb [44]. In the present study, downregulation of endogenous AMPK by target-specific siRNA abolishes PIO-mediated accumulation of $p27^{Kip1}$ (a cell cycle inhibitor) [43], but does not prevent PIO inhibition of PDGF-induced cyclin D1 expression. Together, these findings reveal that PIO has the potential to inhibit VSMC proliferation through AMPK-dependent and AMPK-independent mechanisms beyond its role as a PPARγ agonist. Furthermore, AMPK activation by AICAR results in increased p53 phosphorylation/expression and $p21^{Cip1}$ expression, which in turn inhibits Rb phosphorylation to suppress VSMC proliferation [44]. The present findings reveal that PIO does not affect p53 phosphorylation/expression but it decreases $p21^{Cip1}$ expression, suggesting that p53-p21 axis may not play an intermediary role in PIO inhibition of VSMC proliferation.

Studies with AICAR and adipokines have shown that AMPK activation is associated with diminished ERK activation [25, 33, 34], which in turn is attributable to the suppression of VSMC proliferation [25, 34]. However, there is no apparent causal link between the

observed AMPK activation and diminished ERK phosphorylation toward PIO inhibition of VSMC proliferation (present study). For instance, while AICAR activates AMPK and inhibits agonist-induced ERK phosphorylation [25, 33], overexpression of dominant-negative AMPK abrogates the downstream signal (e.g., ACC phosphorylation) and augments agonist-induced ERK phosphorylation to promote VSMC proliferation [25]. In addition, adipokines such as omentin and adiponectin activate AMPK to inhibit ERK phosphorylation in VSMCs [33, 34]. In particular, genetic blockade of AMPK activation prevents omentin inhibition of PDGF-induced ERK phosphorylation to restore VSMC proliferation [34]. In contrast to AICAR and the aforementioned adipokines, the present findings show that PIO inhibition of basal ERK phosphorylation remains essentially the same after AMPK downregulation and the associated abrogation of ACC phosphorylation. This is further supported by the persistent decrease in PDGF-induced cyclin D1 expression by PIO after AMPK downregulation, thereby suggesting that PIO inhibition of VSMC proliferation occurs in part through mechanisms independent of AMPK activation.

Several lines of evidence suggest that AMPK activation results in the inhibition of mTOR/p70S6K signaling (and *vice versa*) in different tissues/cell types [35, 36], including VSMCs [37]. In particular, AMPK activation in nonvascular cells promotes raptor phosphorylation to inhibit the activity of mTOR [38], a key signaling component that regulates protein synthesis [53, 54], cell cycle progression and cell proliferation [55]. Recent studies with VSMCs demonstrate that ectopic expression of retinoic acid receptor-related orphan receptor-α (RORα) enhances AMPK phosphorylation to inhibit mTOR/p70S6K phosphorylation, thereby suppressing VSMC proliferation [37]. The present findings reveal that PIO not only activates AMPK but also promotes raptor phosphorylation to inhibit mTOR signaling (e.g., ↓ phosphorylation of p70S6K, 4E-BP1, and S6) and protein synthesis in VSMCs. This novel observation is supported by AMPK downregulation studies using target-specific siRNA. Importantly, downregulation of AMPK diminishes PIO-mediated phosphorylation of ACC and raptor, thereby restoring S6 phosphorylation with an accompanying blockade in the accumulation of $p27^{Kip1}$ (a cell cycle inhibitor) [43]. Together, these findings suggest that, in addition to strategies that overexpress RORα in VSMCs [37], treatment with PIO may provide another promising approach to attenuate exaggerated VSMC growth through ↑AMPK → ↓mTOR axis.

While the present findings with PIO point toward AMPK-independent (*via* ↓ ERK) and AMPK-dependent (*via* ↓ mTOR/p70S6K) mechanisms to suppress VSMC proliferation, it is critically important to know whether PPARγ regulates these signaling events. Previously, loss-of-function studies (e.g., dominant-negative PPARγ mutation that suppresses endogenous PPARγ function) have revealed exaggerated neointima formation in mice but without any changes in growth factor-induced ERK phosphorylation, suggesting that endogenous PPARγ does not regulate ERK activation during VSMC proliferation [56]. In a different study, rosiglitazone inhibits PDGF- or arterial injury-induced ERK activation in a PPARγ-independent manner, as evidenced by the use of dominant-negative PPARγ mutant [18]. In conformity with these earlier findings, the present study demonstrates that PIO, while upregulating PPARγ expression in the nucleus, exerts an inhibitory effect on ERK phosphorylation and cyclin D1 expression. Importantly, PIO inhibition of ERK

phosphorylation and cyclin D1 expression is unaffected after PPARγ downregulation (~87%) by target-specific siRNA. Since the contribution of ~13% residual PPARγ expression (in PPARγ siRNA-treated VSMCs) cannot be fully excluded, we employed an additional approach involving VSMC treatment with GW-9662. Pharmacological inhibition of PPARγ by GW-9662 yielded results similar to that observed in PPARγ siRNA-treated VSMCs. Together, these studies suggest that PIO inhibition of key proliferative signaling events (e.g., pERK and cyclin D1) occurs by mechanisms independent of PPARγ in VSMCs. It is noteworthy that the basal ERK phosphorylation in vascular cells is mediated in part by reactive oxygen species (ROS), including superoxide (O_2^-) [57, 58]. In addition, PIO has been shown to inhibit NADPH oxidase-mediated generation of ROS in aortic tissues and VSMCs [59, 60]. Thus, it is likely that PIO inhibits the basal ERK activation by suppressing ROS production in VSMCs.

It is widely accepted that TZD activation of PPARγ in adipocytes results in the synthesis and release of adiponectin [61]. Recent studies demonstrate that exposure of VSMCs to rosiglitazone for 24 hours enhances the expression of adiponectin [62], which in turn can act in an autocrine/paracrine manner to activate AMPK in VSMCs [62, 63]. From the present findings that reveal PIO activation of AMPK, it may therefore be argued that PPARγ-mediated adiponectin synthesis/release is a critical transcriptional event for such an effect. However, our experimental approaches involving siRNA-mediated PPARγ downregulation, chemical inhibition of PPARγ by GW-9662, and time course studies do not support the likely intermediary role of adiponectin toward PIO activation of AMPK in VSMCs. First, neither PPARγ downregulation nor GW-9662 affects PIO activation of AMPK or PIO inhibition of PDGF-induced S6 phosphorylation. Second, PIO activation of AMPK occurs as early as 1 to 3 hours (present study) in contrast to a much longer time frame (≥ 24 hr) that is required for adiponectin upregulation and subsequent AMPK activation [62, 63] in VSMCs. Third, PIO is several fold less potent than rosiglitazone as a PPARγ activator [23]. Together, these studies suggest that PIO activation of AMPK occurs by PPARγ- and adiponectin-independent mechanisms in VSMCs.

TZD derivative(s) have been shown to activate AMPK through ↓ mitochondrial respiratory chain complex I [46], ↓ mitochondrial membrane potential [30], ↑AMP/ATP ratio [28, 29], and/or LKB1 [32] in insulin-responsive tissues and HeLa cells. In particular, ROSI but not PIO at 10 μM and 30 μM concentrations significantly inhibits respiratory complex I enzyme activity in rat skeletal muscle and liver [46], suggesting that PIO activation of AMPK in VSMCs may not involve inhibition of respiratory complex I. Although TRO has been shown to activate AMPK by acutely reducing mitochondrial membrane potential in skeletal muscle cells [30], the present findings from TMRM fluorescence studies do not support the possibility for mitochondrial membrane depolarization by PIO as a likely intermediary event in VSMCs *at least* under the chosen time intervals. In view of the critical link between ↑AMP/ATP ratio and AMPK activation [28, 29], we have also analyzed adenine nucleotide levels in PIO-treated VSMCs. While ROSI at 200 μM concentration increases AMP/ATP ratio in skeletal muscle cells [28], PIO treatment in VSMCs shows a trend toward ↑AMP/ATP ratio but without statistical significance. Given that LKB1 is a catalytic enzyme, the contribution of ~14% residual LKB1 protein (in LKB1 siRNA-treated VSMCs) cannot

be fully excluded with regard to AMPK activation. Furthermore, PIO treatment enhances the phosphorylation of ACC, a key downstream target of AMPK [39] prior to AMPKα^{Thr172} phosphorylation in VSMCs as revealed in our time course study. This may be attributed to an apparent allosteric activation of AMPK without AMPKα^{Thr172} phosphorylation as has been evidenced previously in human melanoma cells upon treatment with A769662, a direct AMPK activator that does not increase intracellular AMP or ADP levels [64]. Future studies are clearly warranted that should compare the role of PIO *versus* ROSI/TRO toward inducing temporal changes in mitochondrial function, including the potential inhibitory effects on mitochondrial pyruvate carrier [65], to identify the upstream signaling events critical for PIO activation of AMPK in VSMCs.

From a clinical standpoint, the findings from the meta-analysis of randomized trials suggest that, in comparison with rosiglitazone that may increase the risk of ischemic events, PIO has a more favorable effect on ischemic vascular complications [66]. PROactive study (PROspective pioglitAzone Clinical Trial In macroVascular Events) reveals that PIO treatment is associated with improved cardiovascular outcomes in patients with type 2 diabetes and macrovascular disease [67]. Nevertheless, the precise mechanisms for such vasoprotective effects remain largely unknown due to the pleiotropic actions of PIO. Notably, PIO has been shown to lower blood pressure [68] and improve endothelial function [68]. It also exhibits anti-inflammatory [69], anti-migratory [70], and anti-proliferative [3] effects in VSMCs. The concentration of PIO used in the present *in vitro* study with VSMCs is nearly one order of magnitude higher than the peak plasma concentration (~3 μM) observed in human subjects on PIO treatment [71]. At this juncture, it is important to note that in comparison with the inhibitory effects of 10-30 μM PIO added directly to VSMCs in culture (present findings and previous studies) [72], a pronounced inhibition of VSMC proliferation occurs upon *in vitro* addition of serum samples obtained from PIO-treated type 2 diabetic subjects [72]. These data suggest that, under *in vivo* conditions, circulating PIO has the potential to exert direct and indirect inhibitory effects on VSMC proliferation. The indirect inhibitory effects of PIO may be attributable to its role in anti-inflammatory action and enhanced adiponectin release. It is well accepted that PIO activation of PPARγ in adipose tissue would enhance circulatory levels of adiponectin [61], which in turn would suppress neointima formation [73] through AMPK activation in VSMCs [62, 63]. The present findings suggest a yet another mechanism for PIO inhibition of VSMC proliferation through AMPK-dependent and AMPK-independent signaling mechanisms regardless of PPARγ expression. Notably, AMPK activation by AICAR has been shown to inhibit neointima formation in balloon-injured rat carotid artery [52]. Recent studies demonstrate that AICAR and metformin inhibit the differentiation of monocytes to macrophages through AMPKα1 activation *in vitro* [74]. In addition, oral administration of metformin attenuates atherosclerotic lesion by inhibiting macrophage accumulation in apoE-deficient mouse aorta [74]. Future studies should compare the effects of therapeutically relevant concentration of PIO *versus* metformin/AICAR on neointima formation after arterial injury in AMPKα1-deficient mice.

In conclusion, PIO has the potential to inhibit VSMC proliferation through indirect effects involving adiponectin/AMPK [61-63, 73], and in part through direct effects involving AMPK-dependent and AMPK-independent regulation of cell cycle regulatory proteins.

Acknowledgements

This work was supported by the National Heart, Lung, and Blood Institute/National Institutes of Health Grant (R01-HL-097090), University of Georgia Research Foundation Fund, and University of Georgia College of Pharmacy Graduate Assistantship Award.

References

[1]. Ross R. Atherosclerosis--an inflammatory disease. N Engl J Med. 1999; 340:115–26. [PubMed: 9887164]

[2]. Owens GK, Kumar MS, Wamhoff BR. Molecular regulation of vascular smooth muscle cell differentiation in development and disease. Physiol Rev. 2004; 84:767–801. [PubMed: 15269336]

[3]. Yoshimoto T, Naruse M, Shizume H, Naruse K, Tanabe A, Tanaka M, et al. Vasculo-protective effects of insulin sensitizing agent pioglitazone in neointimal thickening and hypertensive vascular hypertrophy. Atherosclerosis. 1999; 145:333–40. [PubMed: 10488961]

[4]. Phillips JW, Barringhaus KG, Sanders JM, Yang Z, Chen M, Hesselbacher S, et al. Rosiglitazone reduces the accelerated neointima formation after arterial injury in a mouse injury model of type 2 diabetes. Circulation. 2003; 108:1994–9. [PubMed: 14517165]

[5]. Satoh N, Ogawa Y, Usui T, Tagami T, Kono S, Uesugi H, et al. Antiatherogenic effect of pioglitazone in type 2 diabetic patients irrespective of the responsiveness to its antidiabetic effect. Diabetes Care. 2003; 26:2493–9. [PubMed: 12941708]

[6]. Kahn SE, Haffner SM, Heise MA, Herman WH, Holman RR, Jones NP, et al. Glycemic durability of rosiglitazone, metformin, or glyburide monotherapy. N Engl J Med. 2006; 355:2427–43. [PubMed: 17145742]

[7]. Nesto RW, Bell D, Bonow RO, Fonseca V, Grundy SM, Horton ES, et al. Thiazolidinedione use, fluid retention, and congestive heart failure: a consensus statement from the American Heart Association and American Diabetes Association. October 7, 2003. Circulation. 2003; 108:2941–8. [PubMed: 14662691]

[8]. Guan Y, Hao C, Cha DR, Rao R, Lu W, Kohan DE, et al. Thiazolidinediones expand body fluid volume through PPARgamma stimulation of ENaC-mediated renal salt absorption. Nature Med. 2005; 11:861–6. [PubMed: 16007095]

[9]. Zhang H, Zhang A, Kohan DE, Nelson RD, Gonzalez FJ, Yang T. Collecting duct-specific deletion of peroxisome proliferator-activated receptor gamma blocks thiazolidinedione-induced fluid retention. Proc Natl Acad Sci U S A. 2005; 102:9406–11. [PubMed: 15956187]

[10]. Staels B, Koenig W, Habib A, Merval R, Lebret M, Torra IP, et al. Activation of human aortic smooth-muscle cells is inhibited by PPARalpha but not by PPARgamma activators. Nature. 1998; 393:790–3. [PubMed: 9655393]

[11]. Law RE, Goetze S, Xi XP, Jackson S, Kawano Y, Demer L, et al. Expression and function of PPARgamma in rat and human vascular smooth muscle cells. Circulation. 2000; 101:1311–8. [PubMed: 10725292]

[12]. Benson S, Wu J, Padmanabhan S, Kurtz TW, Pershadsingh HA. Peroxisome proliferator-activated receptor (PPAR)-gamma expression in human vascular smooth muscle cells: inhibition of growth, migration, and c-fos expression by the peroxisome proliferator-activated receptor (PPAR)-gamma activator troglitazone. Am J Hypertens. 2000; 13:74–82. [PubMed: 10678274]

[13]. Benkirane K, Amiri F, Diep QN, El Mabrouk M, Schiffrin EL. PPAR-gamma inhibits ANG II-induced cell growth via SHIP2 and 4E-BP1. Am J Physiol Heart Circ Physiol. 2006; 290:H390–7. [PubMed: 16155101]

[14]. Peuler JD, Phare SM, Iannucci AR, Hodorek MJ. Differential inhibitory effects of antidiabetic drugs on arterial smooth muscle cell proliferation. Am J Hypertens. 1996; 9:188–92. [PubMed: 8924270]

[15]. Law RE, Meehan WP, Xi XP, Graf K, Wuthrich DA, Coats W, et al. Troglitazone inhibits vascular smooth muscle cell growth and intimal hyperplasia. J Clin Invest. 1996; 98:1897–905. [PubMed: 8878442]

[16]. Wakino S, Kintscher U, Kim S, Yin F, Hsueh WA, Law RE. Peroxisome proliferator-activated receptor gamma ligands inhibit retinoblastoma phosphorylation and G1--> S transition in vascular smooth muscle cells. J Biol Chem. 2000; 275:22435–41. [PubMed: 10801895]

[17]. de Dios ST, Bruemmer D, Dilley RJ, Ivey ME, Jennings GL, Law RE, et al. Inhibitory activity of clinical thiazolidinedione peroxisome proliferator activating receptor-gamma ligands toward internal mammary artery, radial artery, and saphenous vein smooth muscle cell proliferation. Circulation. 2003; 107:2548–50. [PubMed: 12742988]

[18]. Lee CS, Kwon YW, Yang HM, Kim SH, Kim TY, Hur J, et al. New mechanism of rosiglitazone to reduce neointimal hyperplasia: activation of glycogen synthase kinase-3beta followed by inhibition of MMP-9. Arterioscler Thromb Vasc Biol. 2009; 29:472–9. [PubMed: 19201691]

[19]. Subramanian V, Golledge J, Ijaz T, Bruemmer D, Daugherty A. Pioglitazone-induced reductions in atherosclerosis occur via smooth muscle cell-specific interaction with PPAR{gamma}. Circ Res. 2010; 107:953–8. [PubMed: 20798360]

[20]. Zhang LL, Gao CY, Fang CQ, Wang YJ, Gao D, Yao GE, et al. PPARgamma attenuates intimal hyperplasia by inhibiting TLR4-mediated inflammation in vascular smooth muscle cells. Cardiovasc Res. 2011; 92:484–93. [PubMed: 21880694]

[21]. Kaul S, Bolger AF, Herrington D, Giugliano RP, Eckel RH. Thiazolidinedione drugs and cardiovascular risks: a science advisory from the American Heart Association and American College of Cardiology Foundation. Circulation. 2010; 121:1868–77. [PubMed: 20179252]

[22]. Inzucchi SE, Bergenstal RM, Buse JB, Diamant M, Ferrannini E, Nauck M, et al. Management of hyperglycaemia in type 2 diabetes: a patient-centered approach. Position statement of the American Diabetes Association (ADA) and the European Association for the Study of Diabetes (EASD). Diabetologia. 2012; 55:1577–96. [PubMed: 22526604]

[23]. Young PW, Buckle DR, Cantello BC, Chapman H, Clapham JC, Coyle PJ, et al. Identification of high-affinity binding sites for the insulin sensitizer rosiglitazone (BRL-49653) in rodent and human adipocytes using a radioiodinated ligand for peroxisomal proliferator-activated receptor gamma. J Pharmacol Exp Ther. 1998; 284:751–9. [PubMed: 9454824]

[24]. Braun-Dullaeus RC, Mann MJ, Seay U, Zhang L, von Der Leyen HE, Morris RE, et al. Cell cycle protein expression in vascular smooth muscle cells in vitro and in vivo is regulated through phosphatidylinositol 3-kinase and mammalian target of rapamycin. Arterioscler Thromb Vasc Biol. 2001; 21:1152–8. [PubMed: 11451744]

[25]. Nagata D, Takeda R, Sata M, Satonaka H, Suzuki E, Nagano T, et al. AMP-activated protein kinase inhibits angiotensin II-stimulated vascular smooth muscle cell proliferation. Circulation. 2004; 110:444–51. [PubMed: 15262850]

[26]. Zhao Y, Biswas SK, McNulty PH, Kozak M, Jun JY, Segar L. PDGF-induced vascular smooth muscle cell proliferation is associated with dysregulation of insulin receptor substrates. Am J Physiol Cell Physiol. 2011; 300:C1375–85. [PubMed: 21325637]

[27]. Goetze S, Xi XP, Graf K, Fleck E, Hsueh WA, Law RE. Troglitazone inhibits angiotensin II-induced extracellular signal-regulated kinase 1/2 nuclear translocation and activation in vascular smooth muscle cells. FEBS Lett. 1999; 452:277–82. [PubMed: 10386606]

[28]. Fryer LG, Parbu-Patel A, Carling D. The Anti-diabetic drugs rosiglitazone and metformin stimulate AMP-activated protein kinase through distinct signaling pathways. J Biol Chem. 2002; 277:25226–32. [PubMed: 11994296]

[29]. Saha AK, Avilucea PR, Ye JM, Assifi MM, Kraegen EW, Ruderman NB. Pioglitazone treatment activates AMP-activated protein kinase in rat liver and adipose tissue in vivo. Biochem Biophys Res Commun. 2004; 314:580–5. [PubMed: 14733947]

[30]. Konrad D, Rudich A, Bilan PJ, Patel N, Richardson C, Witters LA, et al. Troglitazone causes acute mitochondrial membrane depolarisation and an AMPK-mediated increase in glucose phosphorylation in muscle cells. Diabetologia. 2005; 48:954–66. [PubMed: 15834551]

[31]. Coletta DK, Sriwijitkamol A, Wajcberg E, Tantiwong P, Li M, Prentki M, et al. Pioglitazone stimulates AMP-activated protein kinase signalling and increases the expression of genes involved in adiponectin signalling, mitochondrial function and fat oxidation in human skeletal muscle in vivo: a randomised trial. Diabetologia. 2009; 52:723–32. [PubMed: 19169664]

[32]. Boyle JG, Logan PJ, Ewart MA, Reihill JA, Ritchie SA, Connell JM, et al. Rosiglitazone stimulates nitric oxide synthesis in human aortic endothelial cells via AMP-activated protein kinase. J Biol Chem. 2008; 283:11210–7. [PubMed: 18303014]

[33]. Motobayashi Y, Ishizawa Y, Ishizawa K, Orino S, Yamaguchi K, Kawazoe K, et al. Adiponectin inhibits insulin-like growth factor-1-induced cell migration by the suppression of extracellular signal-regulated kinase 1/2 activation, but not Akt in vascular smooth muscle cells. Hypertens Res. 2009; 32:188–93. [PubMed: 19262481]

[34]. Uemura Y, Shibata R, Kanemura N, Ohashi K, Kambara T, Hiramatsu-Ito M, et al. Adipose-derived protein omentin prevents neointimal formation after arterial injury. FASEB J. 2015; 29:141–51. [PubMed: 25300621]

[35]. Inoki K, Kim J, Guan KL. AMPK and mTOR in cellular energy homeostasis and drug targets. Ann Rev Pharmacol Toxicol. 2012; 52:381–400. [PubMed: 22017684]

[36]. Saha AK, Xu XJ, Lawson E, Deoliveira R, Brandon AE, Kraegen EW, et al. Downregulation of AMPK accompanies leucine- and glucose-induced increases in protein synthesis and insulin resistance in rat skeletal muscle. Diabetes. 2010; 59:2426–34. [PubMed: 20682696]

[37]. Kim EJ, Choi YK, Han YH, Kim HJ, Lee IK, Lee MO. RORalpha suppresses proliferation of vascular smooth muscle cells through activation of AMP-activated protein kinase. Int J Cardiol. 2014; 175:515–21. [PubMed: 25017905]

[38]. Gwinn DM, Shackelford DB, Egan DF, Mihaylova MM, Mery A, Vasquez DS, et al. AMPK phosphorylation of raptor mediates a metabolic checkpoint. Mol Cell. 2008; 30:214–26. [PubMed: 18439900]

[39]. Kahn BB, Alquier T, Carling D, Hardie DG. AMP-activated protein kinase: ancient energy gauge provides clues to modern understanding of metabolism. Cell Metab. 2005; 1:15–25. [PubMed: 16054041]

[40]. Pyla R, Poulose N, Jun JY, Segar L. Expression of conventional and novel glucose transporters, GLUT1, -9, -10, and -12, in vascular smooth muscle cells. Am J Physiol Cell Physiol. 2013; 304:C574–89. [PubMed: 23302780]

[41]. Pyla R, Osman I, Pichavaram P, Hansen P, Segar L. Metformin exaggerates phenylephrine-induced AMPK phosphorylation independent of CaMKKbeta and attenuates contractile response in endothelium-denuded rat aorta. Biochem Pharmacol. 2014

[42]. Igarashi M, Hirata A, Yamaguchi H, Tsuchiya H, Ohnuma H, Tominaga M, et al. Characterization of an inhibitory effect of pioglitazone on balloon-injured vascular smooth muscle cell growth. Metabolism. 2001; 50:955–62. [PubMed: 11474485]

[43]. Tanner FC, Boehm M, Akyurek LM, San H, Yang ZY, Tashiro J, et al. Differential effects of the cyclin-dependent kinase inhibitors p27(Kip1), p21(Cip1), and p16(Ink4) on vascular smooth muscle cell proliferation. Circulation. 2000; 101:2022–5. [PubMed: 10790340]

[44]. Igata M, Motoshima H, Tsuruzoe K, Kojima K, Matsumura T, Kondo T, et al. Adenosine monophosphate-activated protein kinase suppresses vascular smooth muscle cell proliferation through the inhibition of cell cycle progression. Circ Res. 2005; 97:837–44. [PubMed: 16151020]

[45]. Yu W, Liu-Bryan R, Stevens S, Damanahalli JK, Terkeltaub R. RAGE signaling mediates post-injury arterial neointima formation by suppression of liver kinase B1 and AMPK activity. Atherosclerosis. 2012; 222:417–25. [PubMed: 22552116]

[46]. Brunmair B, Staniek K, Gras F, Scharf N, Althaym A, Clara R, et al. Thiazolidinediones, like metformin, inhibit respiratory complex I: a common mechanism contributing to their antidiabetic actions? Diabetes. 2004; 53:1052–9. [PubMed: 15047621]

[47]. Ma XM, Blenis J. Molecular mechanisms of mTOR-mediated translational control. Nature Rev Mol Cell Biol. 2009; 10:307–18. [PubMed: 19339977]

[48]. Hardie DG. AMPK and Raptor: matching cell growth to energy supply. Mol Cell. 2008; 30:263–5. [PubMed: 18471972]

[49]. Bishop-Bailey D, Hla T, Warner TD. Intimal smooth muscle cells as a target for peroxisome proliferator-activated receptor-gamma ligand therapy. Circ Res. 2002; 91:210–7. [PubMed: 12169646]

[50]. Nagahama R, Matoba T, Nakano K, Kim-Mitsuyama S, Sunagawa K, Egashira K. Nanoparticle-mediated delivery of pioglitazone enhances therapeutic neovascularization in a murine model of hindlimb ischemia. Arterioscler Thromb Vasc Biol. 2012; 32:2427–34. [PubMed: 22879581]

[51]. Joner M, Morimoto K, Kasukawa H, Steigerwald K, Merl S, Nakazawa G, et al. Site-specific targeting of nanoparticle prednisolone reduces in-stent restenosis in a rabbit model of established atheroma. Arterioscler Thromb Vasc Biol. 2008; 28:1960–6. [PubMed: 18688017]

[52]. Stone JD, Narine A, Shaver PR, Fox JC, Vuncannon JR, Tulis DA. AMP-activated protein kinase inhibits vascular smooth muscle cell proliferation and migration and vascular remodeling following injury. Am J Physiol Heart Circ Physiol. 2013; 304:H369–81. [PubMed: 23203966]

[53]. Sengupta S, Peterson TR, Sabatini DM. Regulation of the mTOR complex 1 pathway by nutrients, growth factors, and stress. Mol Cell. 2010; 40:310–22. [PubMed: 20965424]

[54]. Ning J, Clemmons DR. AMP-activated protein kinase inhibits IGF-I signaling and protein synthesis in vascular smooth muscle cells via stimulation of insulin receptor substrate 1 S794 and tuberous sclerosis 2 S1345 phosphorylation. Mol Endocrinol. 2010; 24:1218–29. [PubMed: 20363874]

[55]. Martinet W, De Loof H, De Meyer GR. mTOR inhibition: a promising strategy for stabilization of atherosclerotic plaques. Atherosclerosis. 2014; 233:601–7. [PubMed: 24534455]

[56]. Meredith D, Panchatcharam M, Miriyala S, Tsai YS, Morris AJ, Maeda N, et al. Dominant-negative loss of PPARgamma function enhances smooth muscle cell proliferation, migration, and vascular remodeling. Arterioscler Thromb Vasc Biol. 2009; 29:465–71. [PubMed: 19179641]

[57]. Li JM, Wheatcroft S, Fan LM, Kearney MT, Shah AM. Opposing roles of p47phox in basal versus angiotensin II-stimulated alterations in vascular O2- production, vascular tone, and mitogen-activated protein kinase activation. Circulation. 2004; 109:1307–13. [PubMed: 14993144]

[58]. Lee KP, Sudjarwo GW, Jung SH, Lee D, Lee DY, Lee GB, et al. Carvacrol inhibits atherosclerotic neointima formation by downregulating reactive oxygen species production in vascular smooth muscle cells. Atherosclerosis. 2015; 240:367–73. [PubMed: 25875388]

[59]. Martin A, Perez-Giron JV, Hernanz R, Palacios R, Briones AM, Fortuno A, et al. Peroxisome proliferator-activated receptor-gamma activation reduces cyclooxygenase-2 expression in vascular smooth muscle cells from hypertensive rats by interfering with oxidative stress. J Hypertens. 2012; 30:315–26. [PubMed: 22179086]

[60]. Perez-Giron JV, Palacios R, Martin A, Hernanz R, Aguado A, Martinez-Revelles S, et al. Pioglitazone reduces angiotensin II-induced COX-2 expression through inhibition of ROS production and ET-1 transcription in vascular cells from spontaneously hypertensive rats. Am J Physiol Heart Circ Physiol. 2014; 306:H1582–93. [PubMed: 24727493]

[61]. Kadowaki T, Yamauchi T, Kubota N, Hara K, Ueki K, Tobe K. Adiponectin and adiponectin receptors in insulin resistance, diabetes, and the metabolic syndrome. J Clin Invest. 2006; 116:1784–92. [PubMed: 16823476]

[62]. Ding M, Carrao AC, Wagner RJ, Xie Y, Jin Y, Rzucidlo EM, et al. Vascular smooth muscle cell-derived adiponectin: a paracrine regulator of contractile phenotype. J Mol Cell Cardiol. 2012; 52:474–84. [PubMed: 21952104]

[63]. Ding M, Xie Y, Wagner RJ, Jin Y, Carrao AC, Liu LS, et al. Adiponectin induces vascular smooth muscle cell differentiation via repression of mammalian target of rapamycin complex 1 and FoxO4. Arterioscler Thromb Vasc Biol. 2011; 31:1403–10. [PubMed: 21454807]

[64]. Gowans GJ, Hawley SA, Ross FA, Hardie DG. AMP is a true physiological regulator of AMP-activated protein kinase by both allosteric activation and enhancing net phosphorylation. Cell Metab. 2013; 18:556–66. [PubMed: 24093679]

[65]. Divakaruni AS, Wiley SE, Rogers GW, Andreyev AY, Petrosyan S, Loviscach M, et al. Thiazolidinediones are acute, specific inhibitors of the mitochondrial pyruvate carrier. Proc Natl Acad Sci U S A. 2013; 110:5422–7. [PubMed: 23513224]

[66]. Lincoff AM, Wolski K, Nicholls SJ, Nissen SE. Pioglitazone and risk of cardiovascular events in patients with type 2 diabetes mellitus: a meta-analysis of randomized trials. JAMA. 2007; 298:1180–8. [PubMed: 17848652]

[67]. Dormandy JA, Charbonnel B, Eckland DJ, Erdmann E, Massi-Benedetti M, Moules IK, et al. Secondary prevention of macrovascular events in patients with type 2 diabetes in the PROactive Study (PROspective pioglitAzone Clinical Trial In macroVascular Events): a randomised controlled trial. Lancet. 2005; 366:1279–89. [PubMed: 16214598]

[68]. Hsueh WA, Law RE. PPARgamma and atherosclerosis: effects on cell growth and movement. Arterioscler Thromb Vasc Biol. 2001; 21:1891–5. [PubMed: 11742860]

[69]. Ishibashi M, Egashira K, Hiasa K, Inoue S, Ni W, Zhao Q, et al. Antiinflammatory and antiarteriosclerotic effects of pioglitazone. Hypertension. 2002; 40:687–93. [PubMed: 12411463]

[70]. Game BA, Maldonado A, He L, Huang Y. Pioglitazone inhibits MMP-1 expression in vascular smooth muscle cells through a mitogen-activated protein kinase-independent mechanism. Atherosclerosis. 2005; 178:249–56. [PubMed: 15694931]

[71]. Hanefeld M. Pharmacokinetics and clinical efficacy of pioglitazone. International Journal of Clinical Practice Supplement. 2001:19–25. [PubMed: 11594240]

[72]. Hong SJ, Kim ST, Kim TJ, Kim EO, Ahn CM, Park JH, et al. Cellular and molecular changes associated with inhibitory effect of pioglitazone on neointimal growth in patients with type 2 diabetes after zotarolimus-eluting stent implantation. Arterioscler Thromb Vasc Biol. 2010; 30:2655–65. [PubMed: 21030718]

[73]. Arita Y, Kihara S, Ouchi N, Maeda K, Kuriyama H, Okamoto Y, et al. Adipocyte-derived plasma protein adiponectin acts as a platelet-derived growth factor-BB-binding protein and regulates growth factor-induced common postreceptor signal in vascular smooth muscle cell. Circulation. 2002; 105:2893–8. [PubMed: 12070119]

[74]. Vasamsetti SB, Karnewar S, Kanugula AK, Thatipalli AR, Kumar JM, Kotamraju S. Metformin inhibits monocyte-to-macrophage differentiation via AMPK-mediated inhibition of STAT3 activation: potential role in atherosclerosis. Diabetes. 2015; 64:2028–41. [PubMed: 25552600]

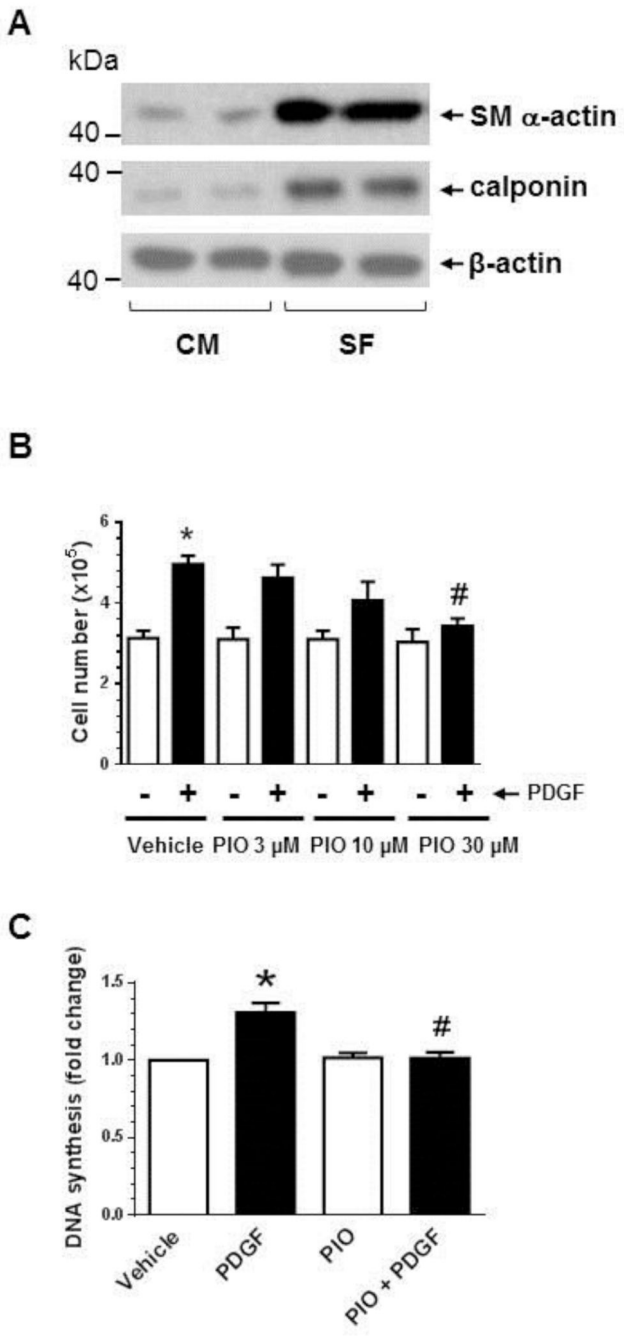

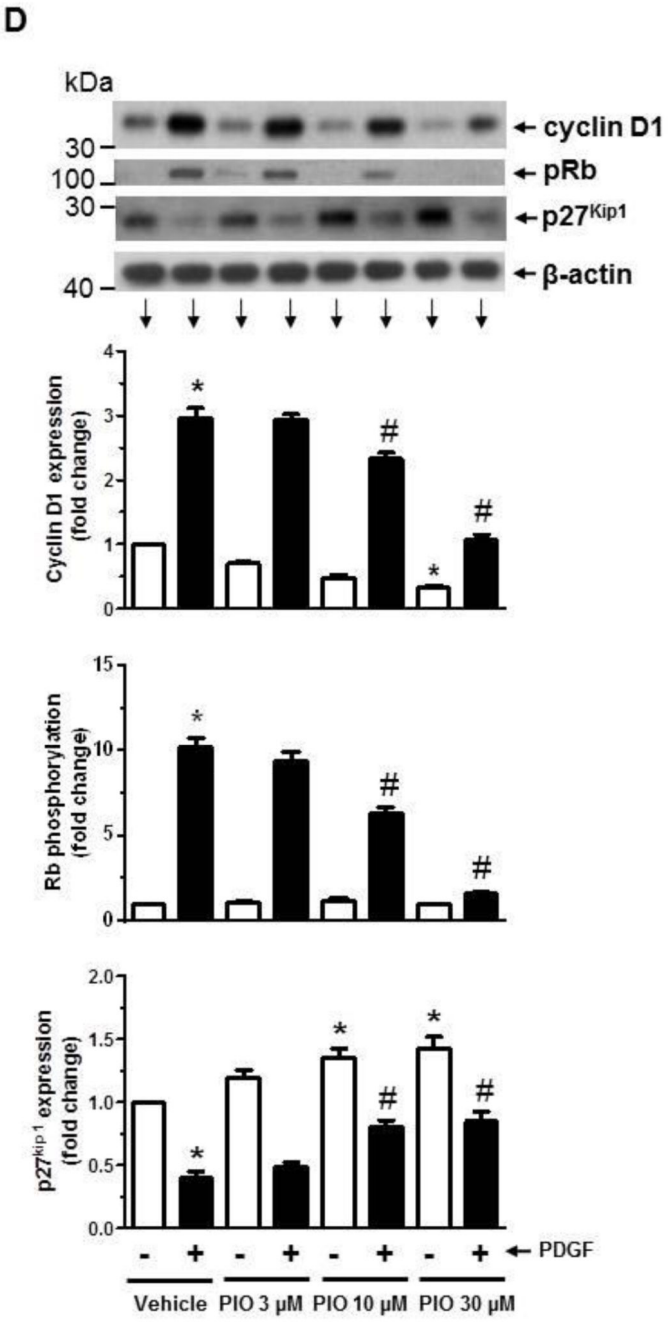

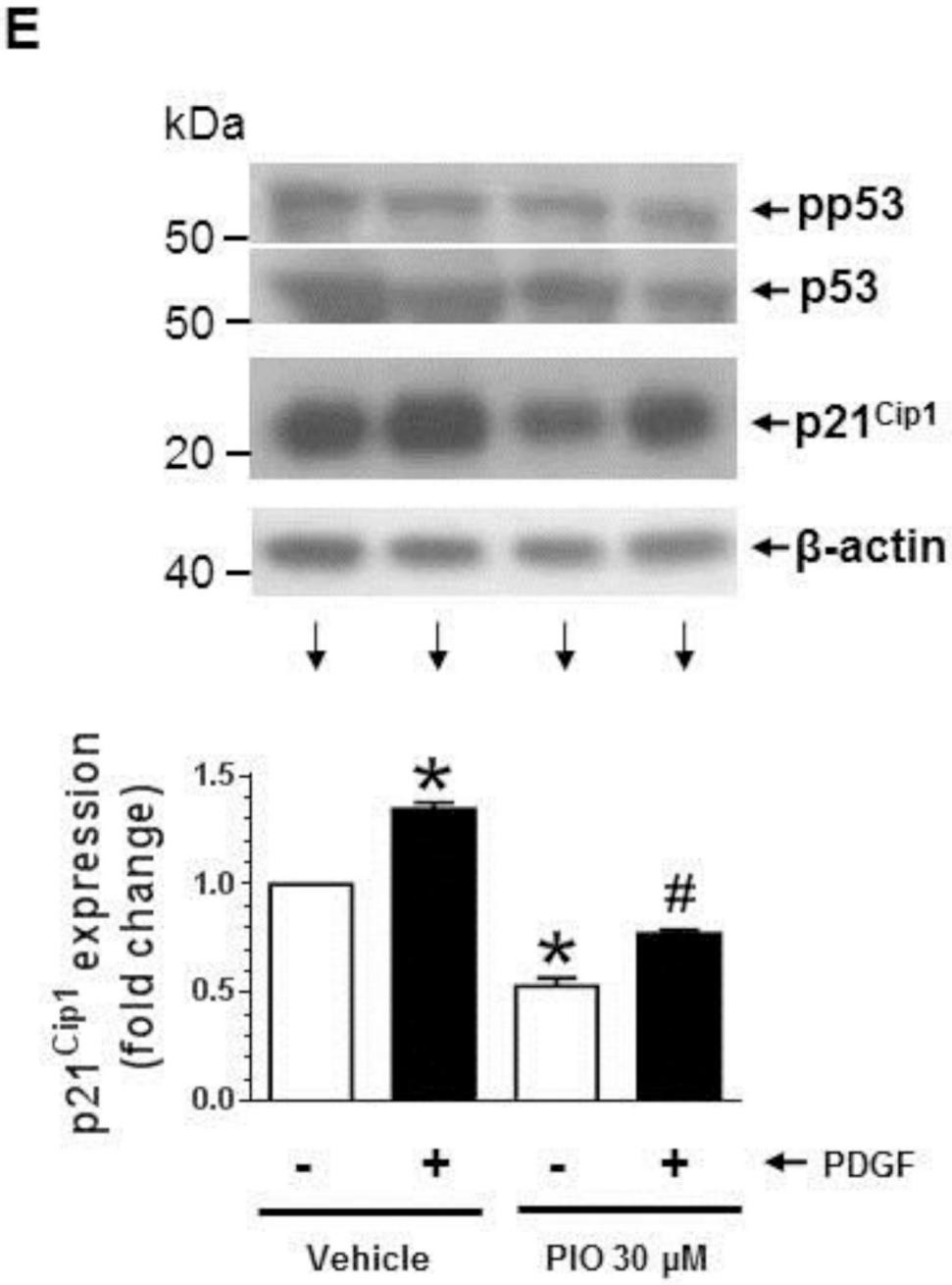

Fig. 1.

Effects of PIO on VSMC proliferation, DNA synthesis, and cell cycle proteins in the absence or presence of PDGF. (**A**) Subconfluent VSMCs were maintained in complete medium (CM) or serum-deprived conditions (SF) for 48 hr. VSMC lysates were then subjected to immunoblot analysis using primary antibodies specific for SM α-actin or calponin. The immunoblots shown are representative of n = 3. (**B**) Serum-deprived VSMCs were pretreated with PIO (3, 10, or 30 μM) or vehicle control for 30 min. This was followed by exposure to PDGF (30 ng/ml) for 96 hr to determine the changes in cell number. (**C**)

Serum-deprived VSMCs were pretreated with PIO (30 μM) or vehicle control for 24 hr, and then exposed to PDGF (30 ng/ml) for 24 hr to determine the changes in DNA synthesis. Serum-deprived VSMCs were pretreated with PIO at the indicated concentrations or vehicle control for 30 min. This was followed by exposure to PDGF (30 ng/ml) for 48 hr to determine the changes in: (**D**) cyclin D1, pRb, and $p27^{Kip1}$; and (**E**) pp53, p53, and $p21^{Cip1}$ by immunoblot analysis. *$p < 0.05$ compared with vehicle control; $^{\#}p < 0.05$ compared with PDGF alone; $n = 3$.

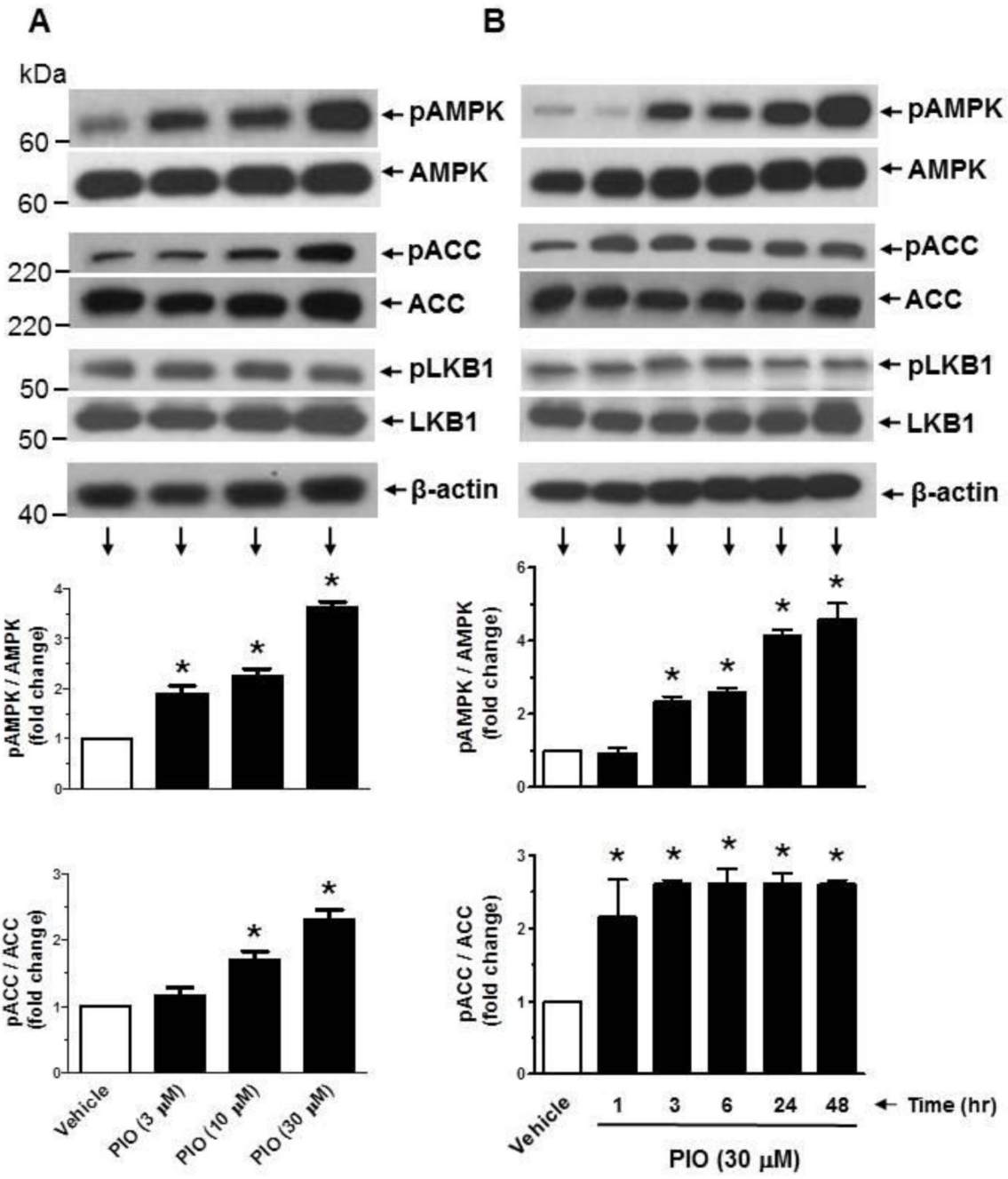

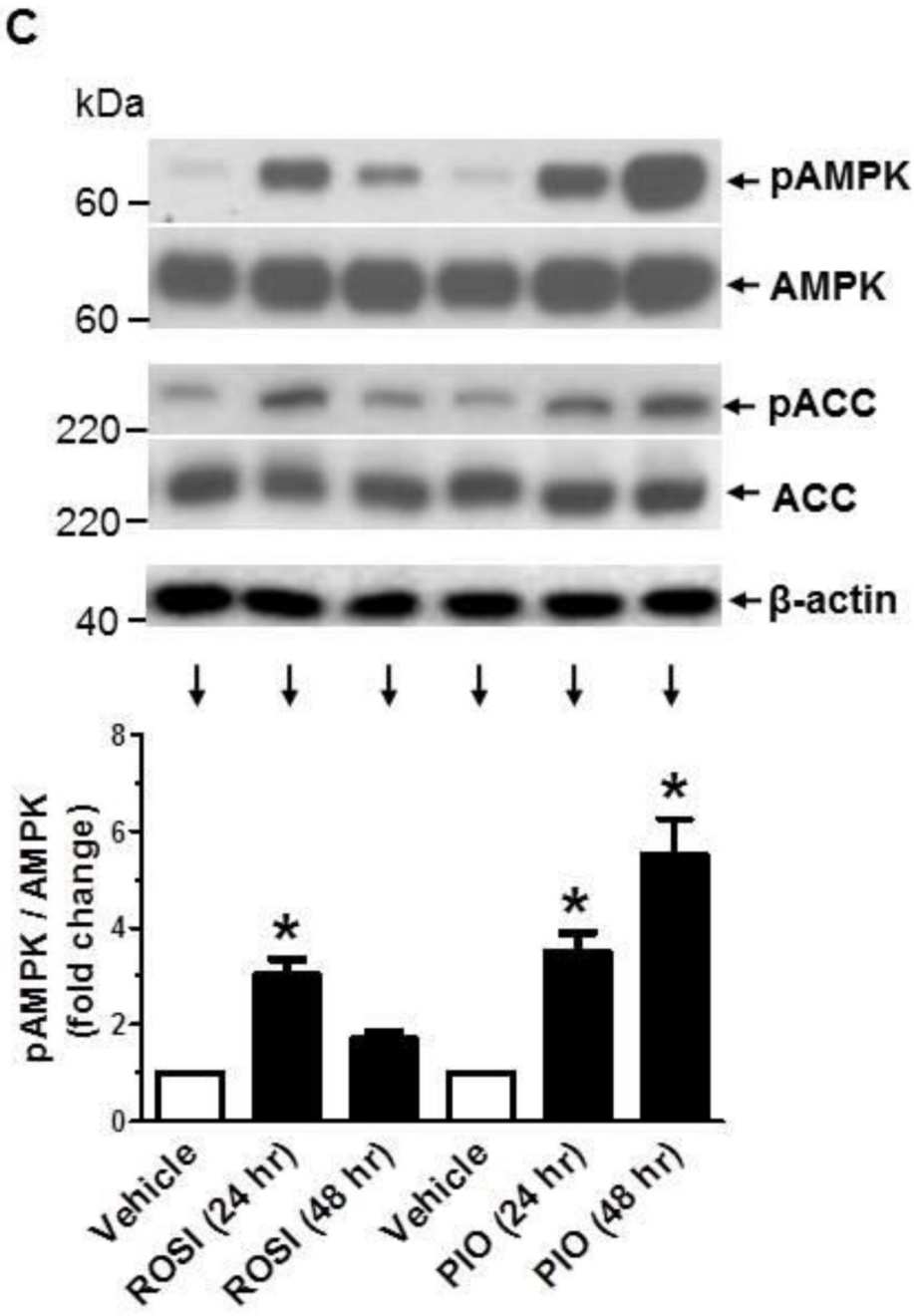

Fig. 2.

Effects of PIO on AMPK and ACC phosphorylation as a function of concentration and time. Serum-deprived VSMCs were treated with increasing concentrations of PIO (3 to 30 μM) or vehicle control for 48 hr (**A**) or a fixed concentration of PIO (30 μM) for 1 to 48 hr (**B**). In addition, serum-deprived VSMCs were exposed to ROSI (30 μM) *versus* PIO (30 μM) for 24 or 48 hr (**C**). VSMC lysates were then subjected to immunoblot analysis using primary antibodies specific for pAMPK, pACC, or pLKB1. *$p < 0.05$ compared with vehicle control; $n = 3$.

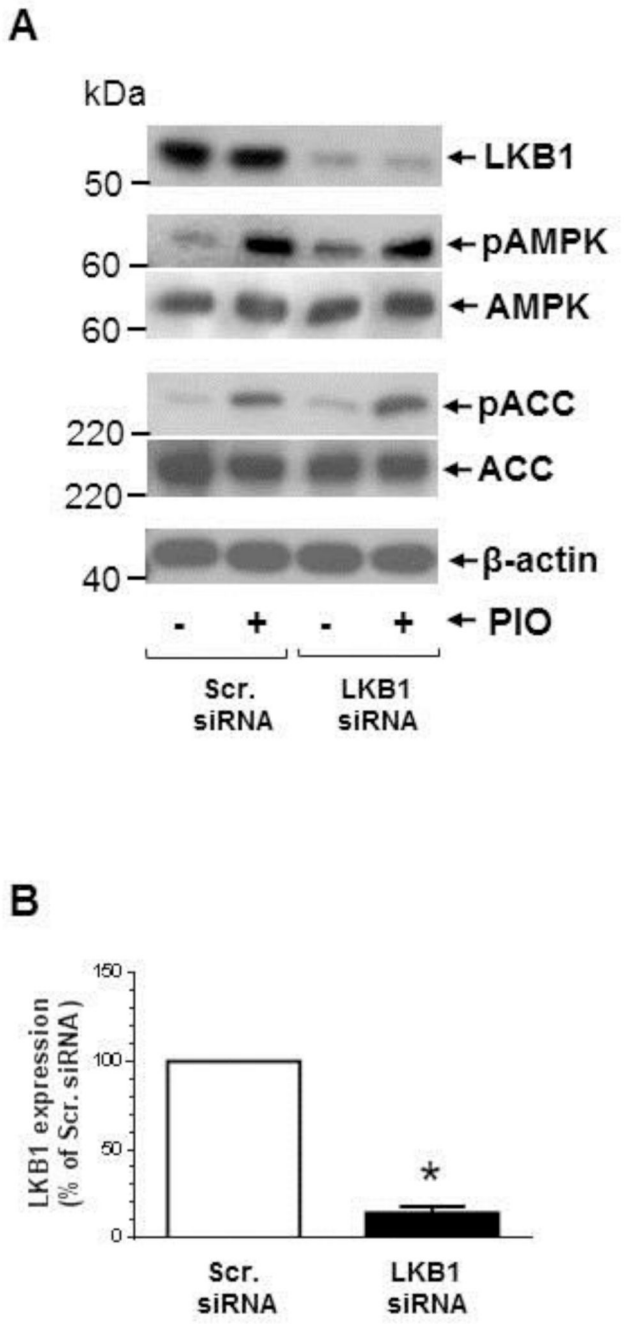

Fig. 3.

Effects of LKB1 downregulation on PIO activation of AMPK in VSMCs. (**A**-**B**) VSMCs were transfected with scrambled (Scr.) or LKB1 siRNA followed by maintenance in culture for 48 hr. Subsequently, VSMCs were treated with PIO (30 μM, 48 hr) or vehicle control under serum-deprived conditions. VSMC lysates were then subjected to immunoblot analysis using primary antibodies specific for LKB1, pAMPK and pACC. *$p < 0.05$ compared with scr. siRNA; immunoblots shown are representative of n = 3.

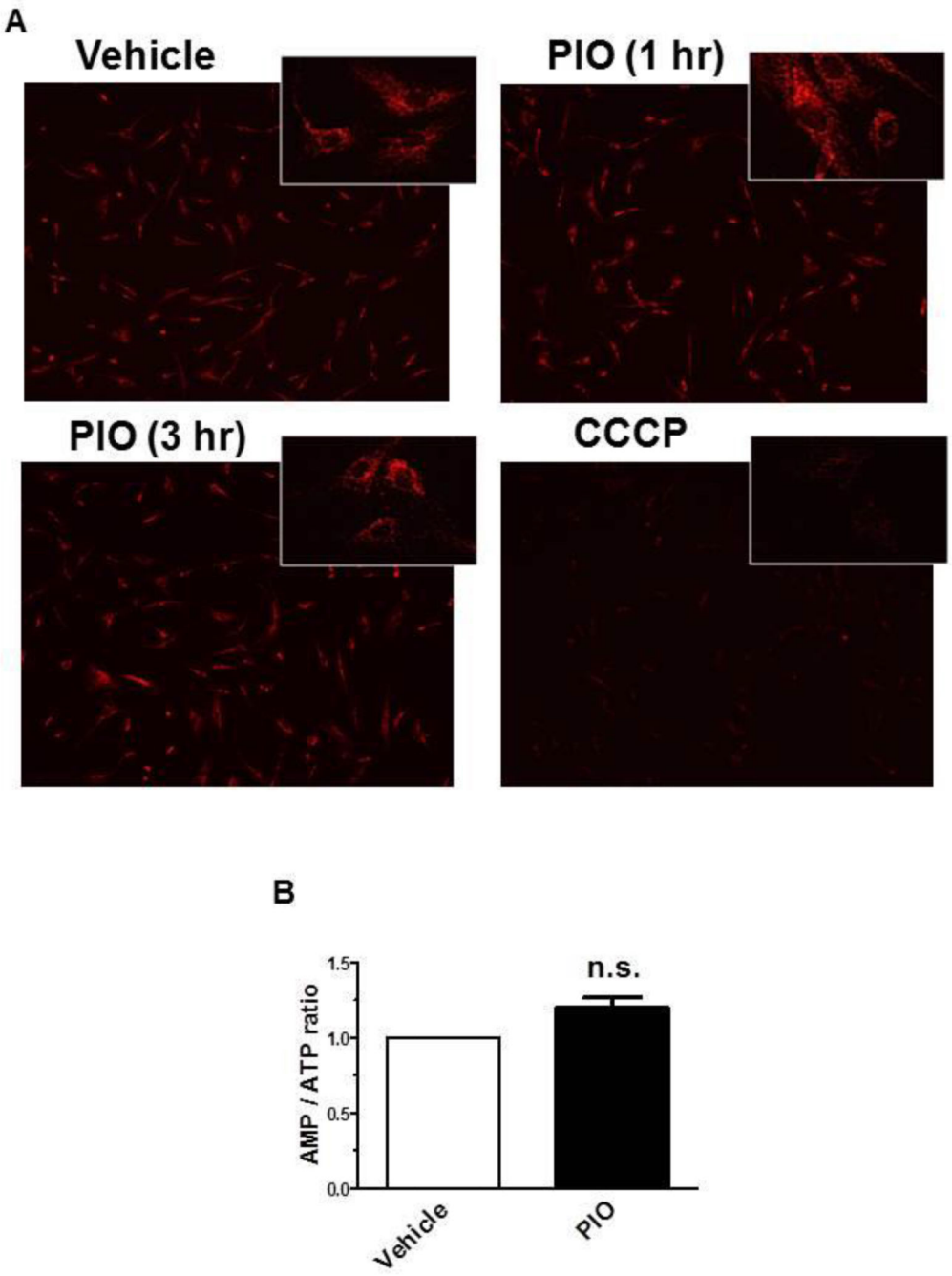

Fig. 4.

Effects of PIO on mitochondrial membrane potential and AMP/ATP ratio in VSMCs. Serum-deprived VSMCs were treated with: (**A**) PIO (30 μM, 1 or 3 hr), CCCP (50 μM, 1 hr), or vehicle control followed by fluorescence microscopy analysis of mitochondrial membrane potential; or (**B**) PIO (30 μM, 3 hr) or vehicle control followed by LC-MS/MS MRM analysis of AMP/ATP ratio. n.s. not significant compared with vehicle control; n = 4.

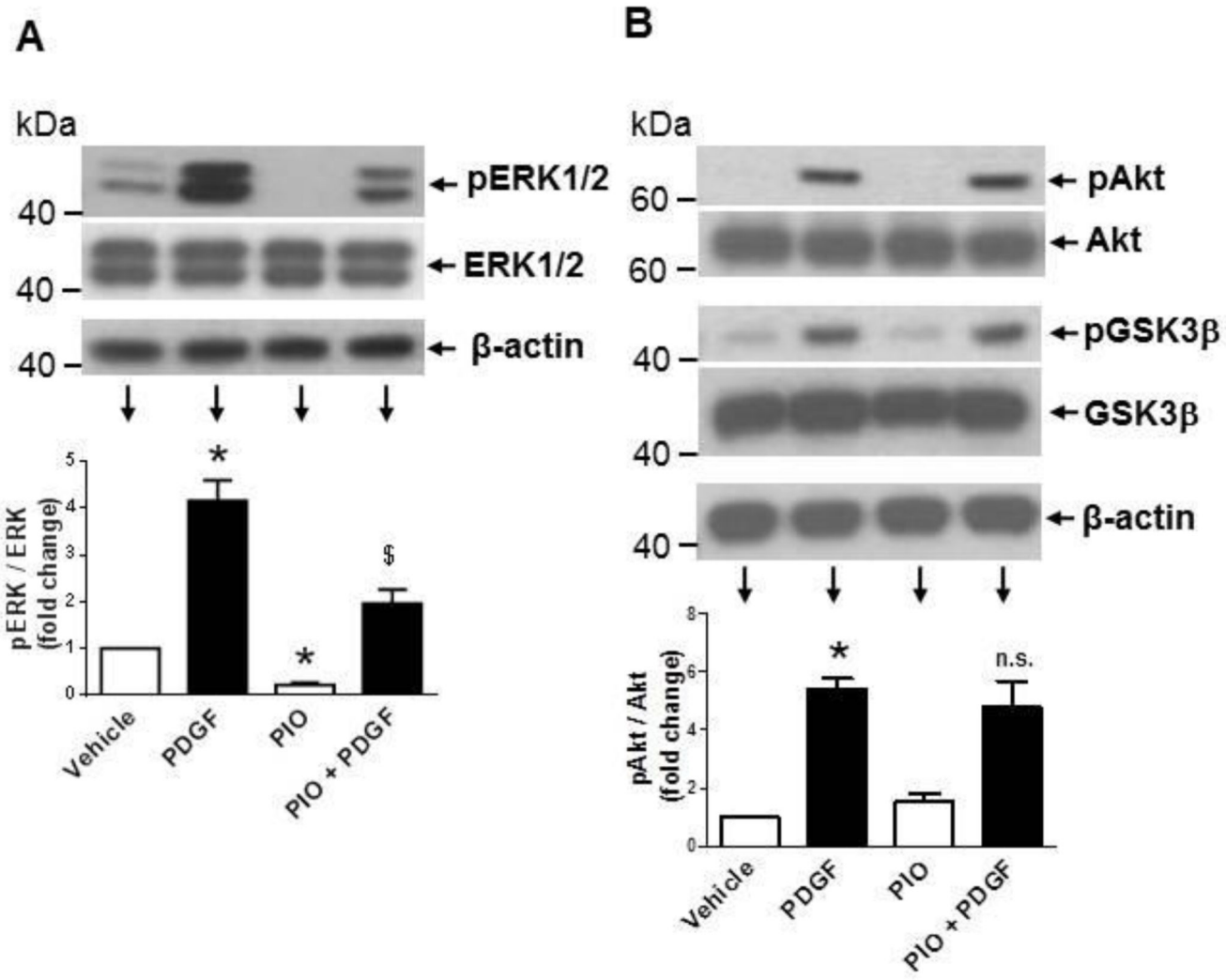

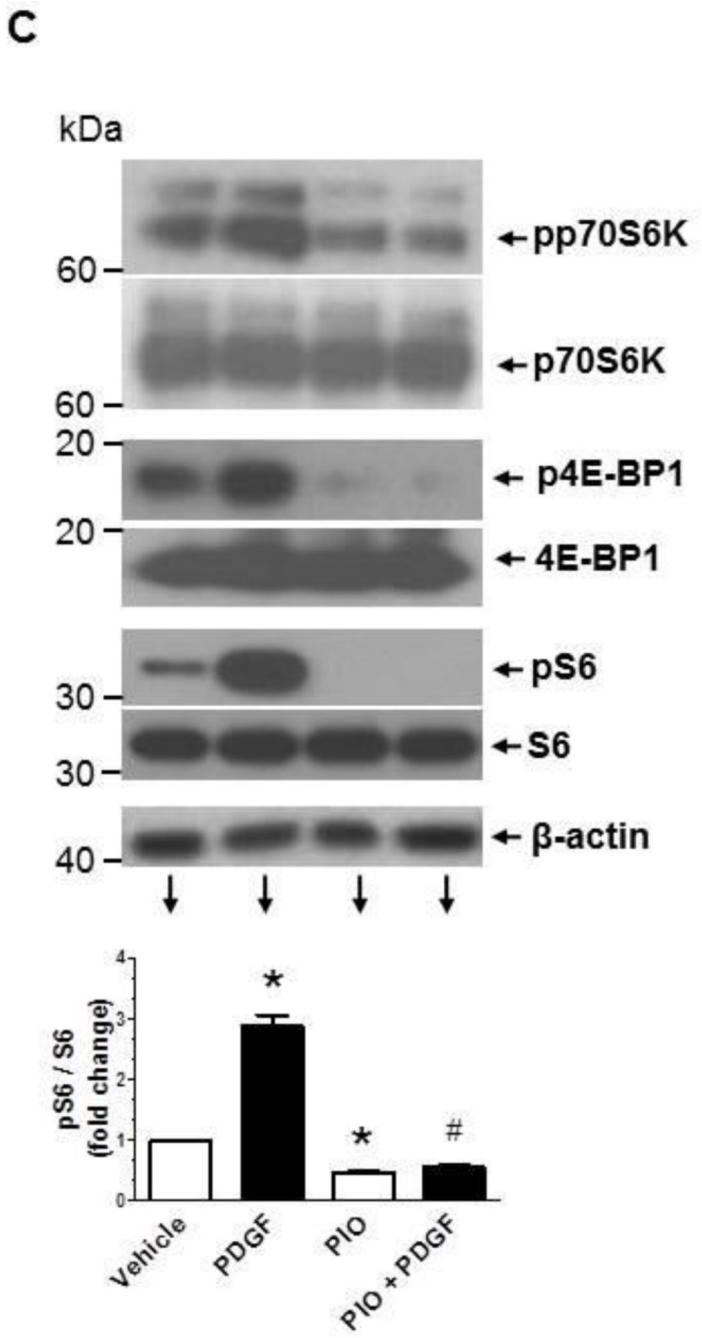

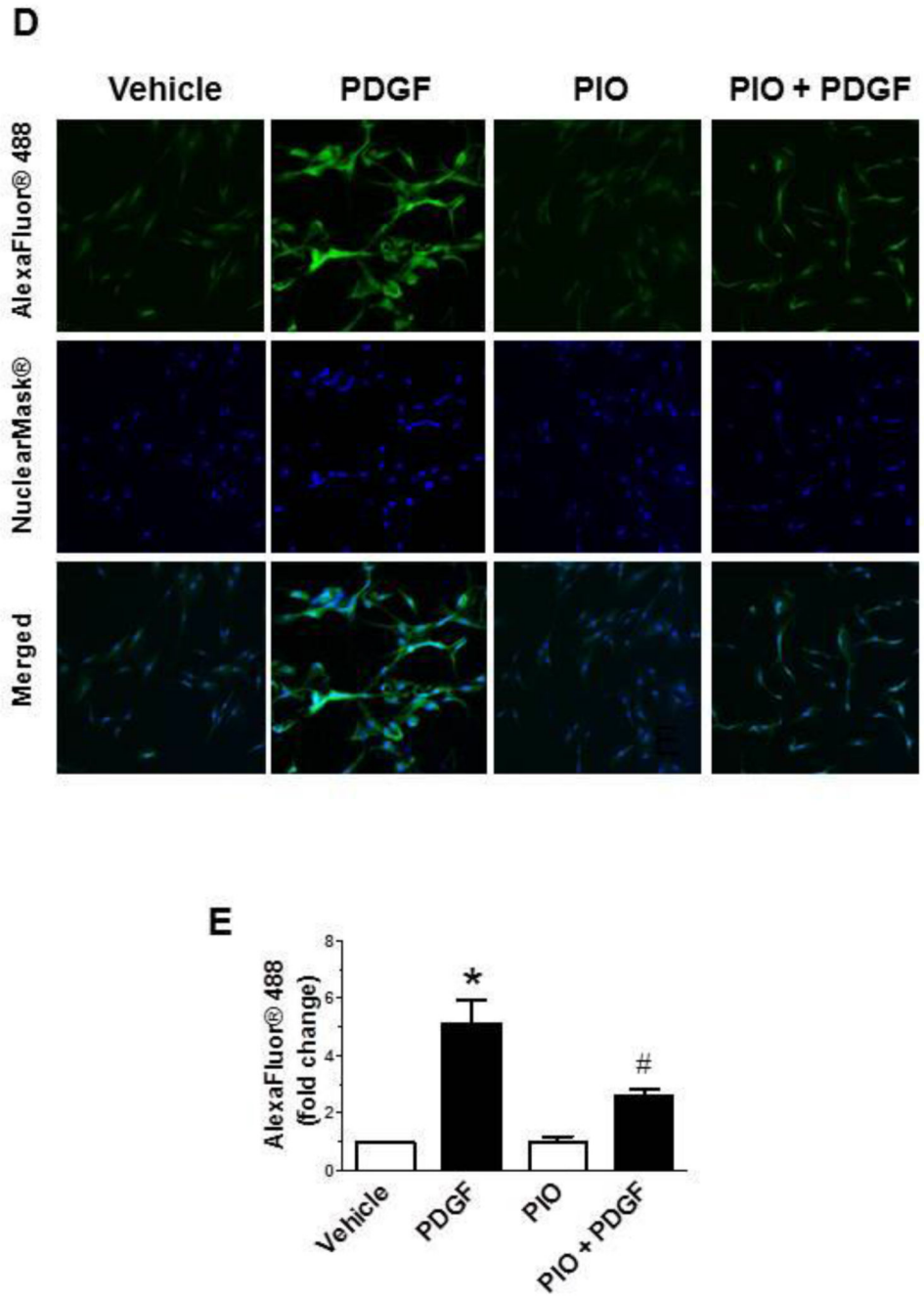

Fig. 5.

Effects of PIO on PDGF-induced signaling events and protein synthesis in VSMCs. Serum-deprived VSMCs were pretreated with PIO (30 μM) or vehicle control for 30 min followed by exposure to: (**A**-**C**) PDGF (30 ng/ml, 48 hr) to determine the changes in protein phosphorylation; or (**D**-**E**) PDGF (30 ng/ml, 24 hr) to determine nascent protein synthesis. For protein phosphorylation, VSMC lysates were subjected to immunoblot analysis using primary antibodies specific for pERK1/2, pAkt, pGSK3β, pp70S6K, p4E-BP1, and pS6. *p

<0.05 compared with vehicle control; $^{\$}p < 0.05$ compared with PIO alone; n.s. not significant compared with PDGF alone; n = 3.

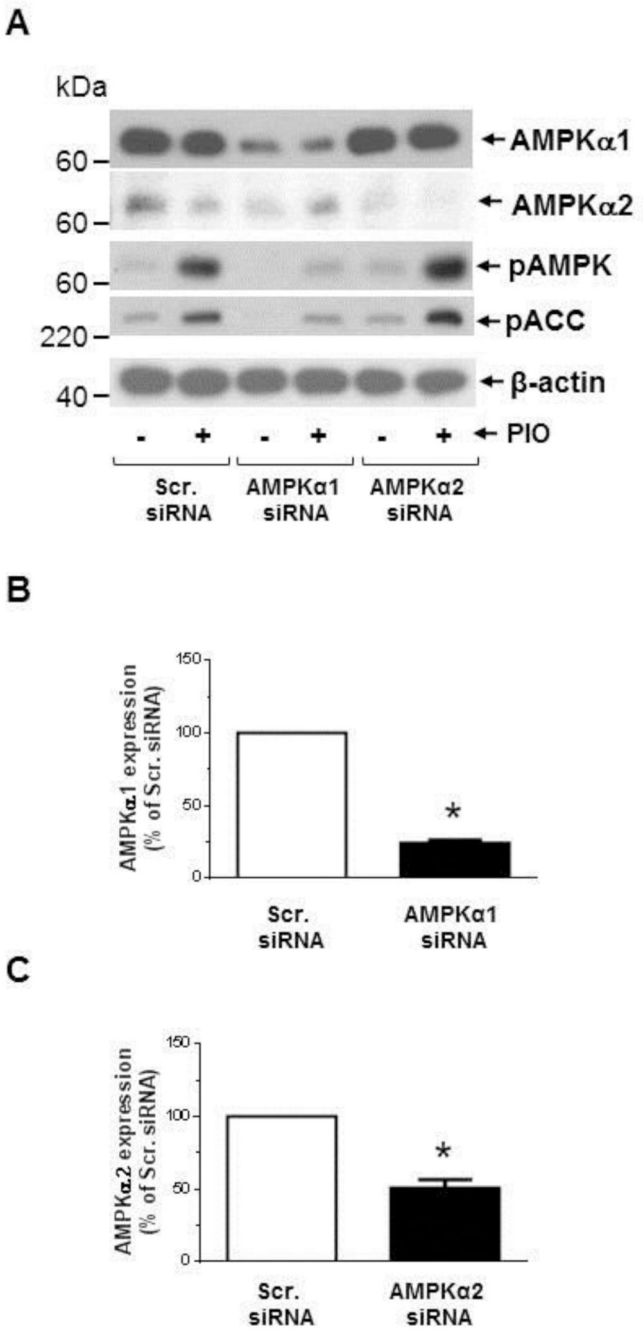

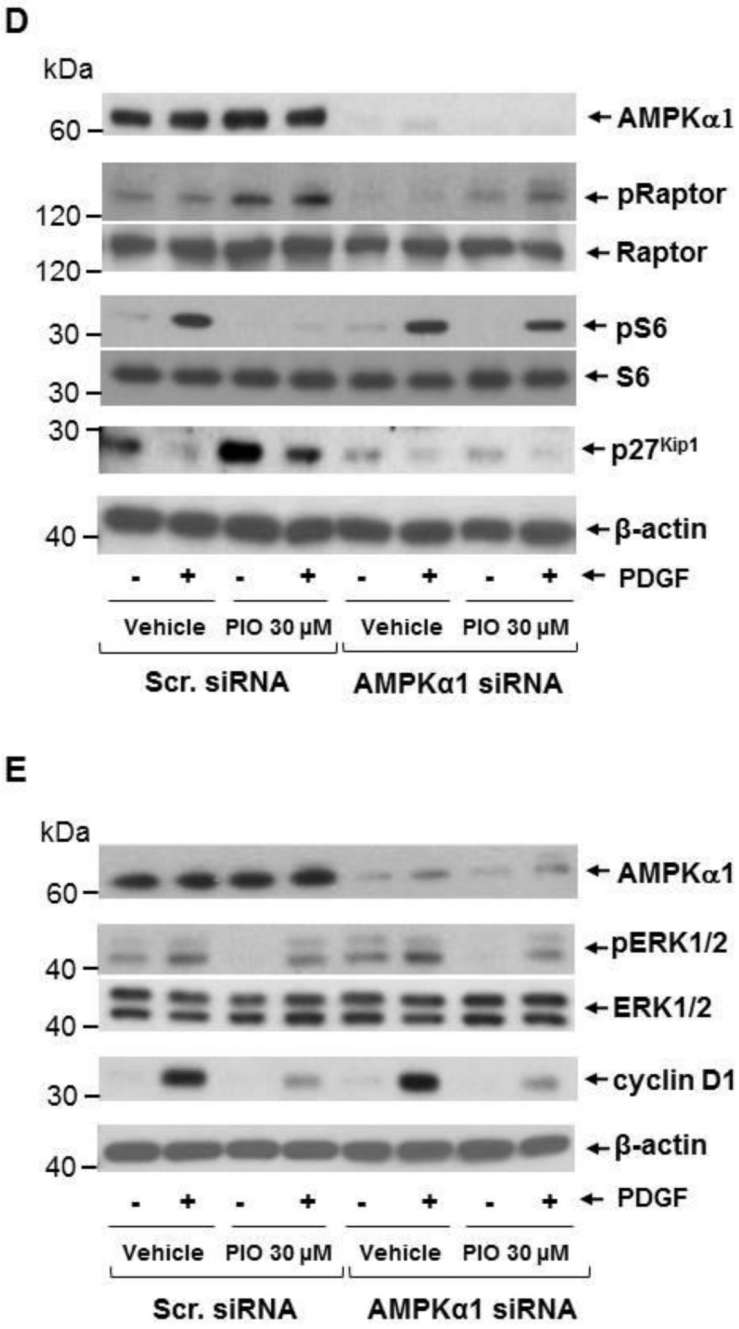

Fig. 6.

Effects of AMPKα1 downregulation on PIO regulation of PDGF-induced signaling events. VSMCs were transfected with scrambled (Scr.), AMPKα1, or AMPKα2 siRNA followed by maintenance in culture for 48 hr. Subsequently, VSMCs were treated with: (**A-C**) PIO (30 μM, 48 hr) or vehicle control under serum-deprived conditions. VSMC lysates were then subjected to immunoblot analysis using primary antibodies specific for AMPKα1, AMPKα2, pAMPK and pACC. *$p < 0.05$ compared with scr. siRNA; or (**D-E**) PIO (30 μM, 30 min) or vehicle control followed by exposure to PDGF (30 ng/ml, 48 hr). VSMC lysates

were then subjected to immunoblot analysis for pRaptor, pS6 and $p27^{kip1}$, pERK1/2, and cyclin D1. Immunoblots shown are representative of n = 3.

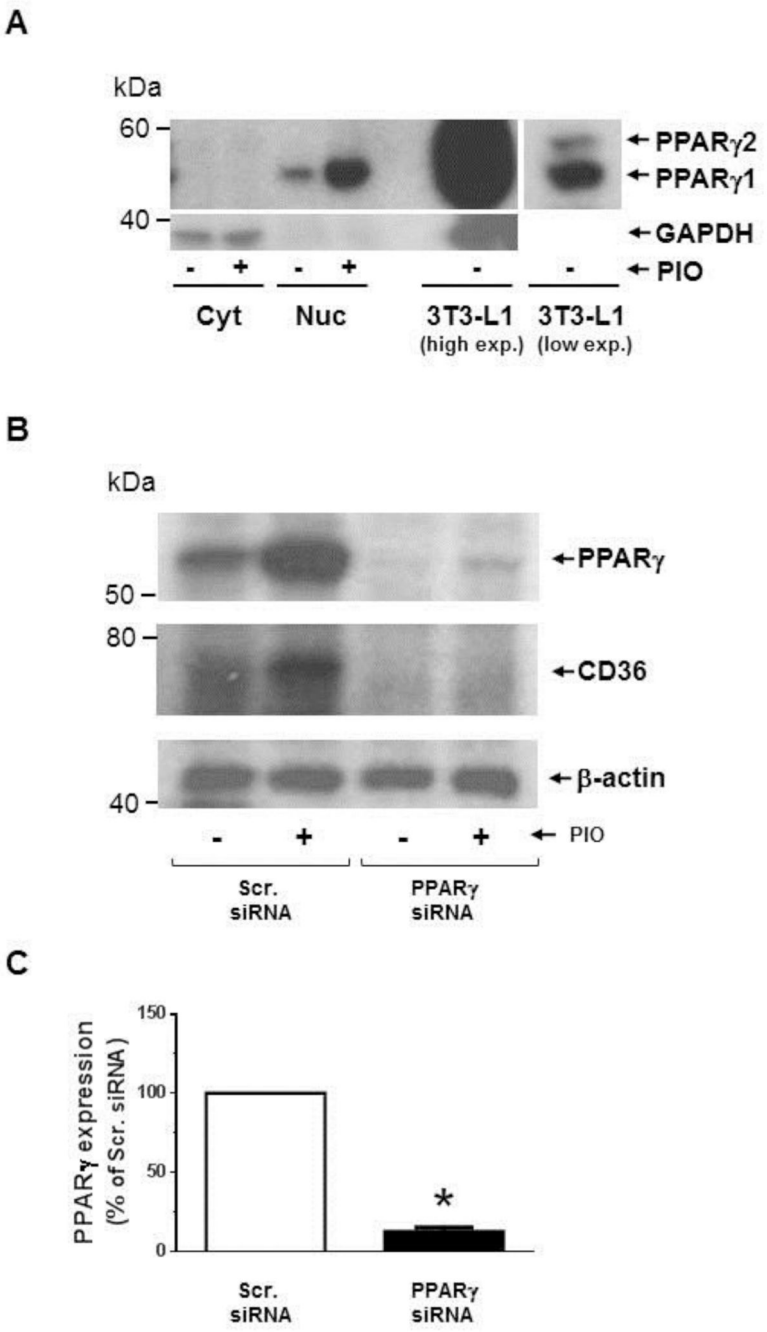

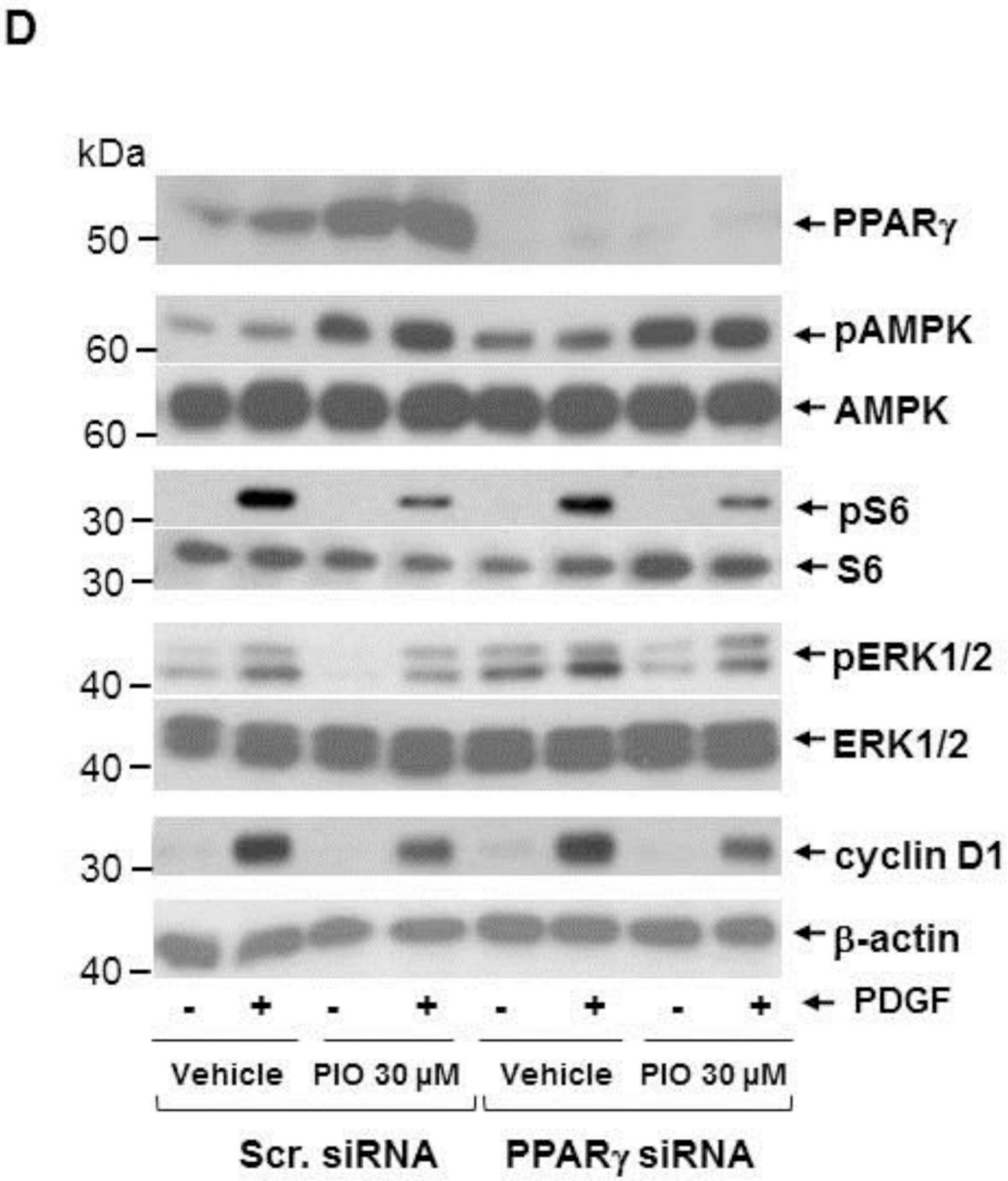

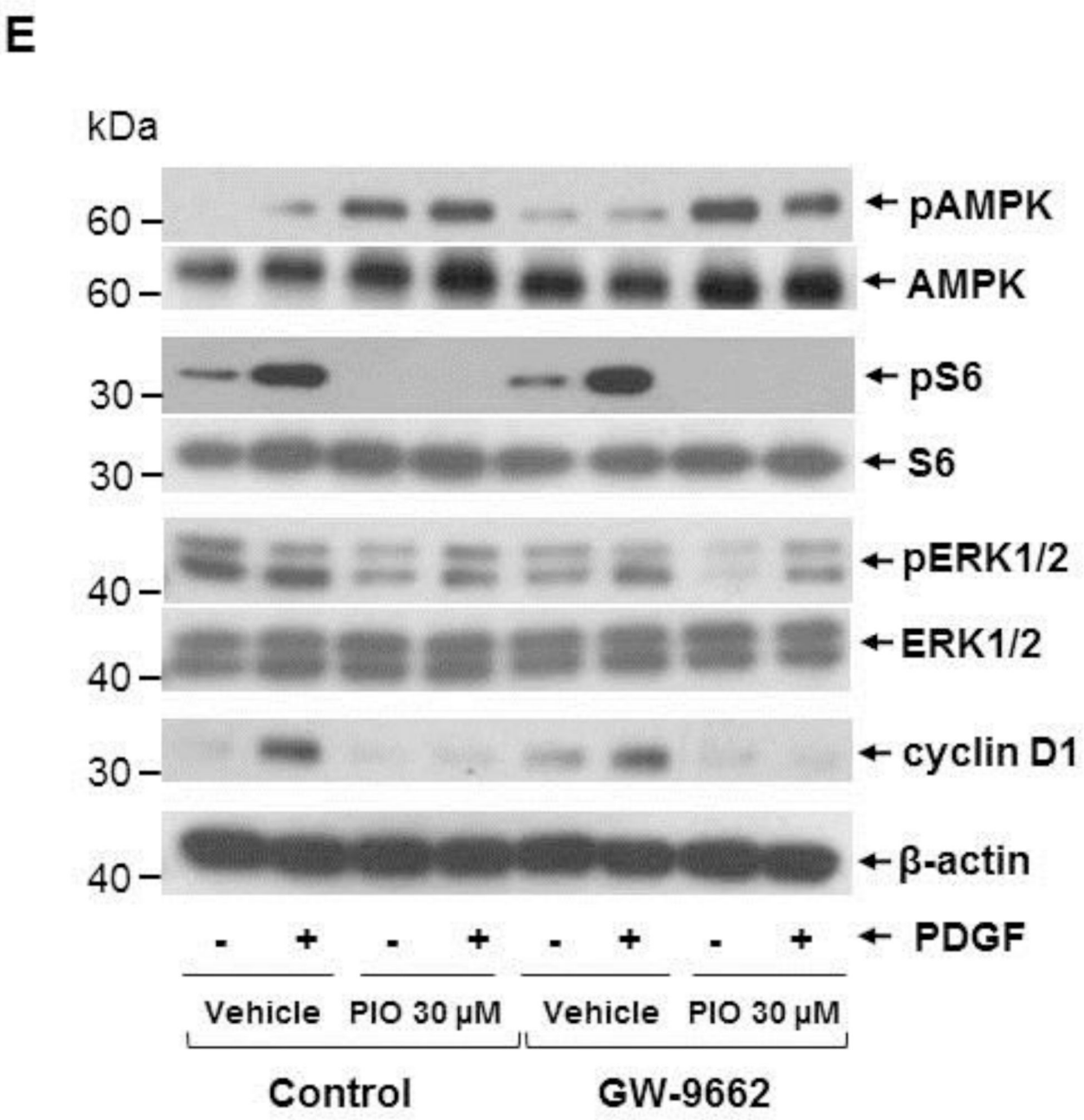

Fig. 7.

Effects of PPARγ downregulation or PPARγ inhibition on PIO-induced changes in the phosphorylation of AMPK, S6, and ERK1/2, and cyclin D1 expression in VSMCs. **(A)** Serum-deprived VSMCs were treated with PIO (30 μM, 48 hr) or vehicle control. Subsequently, nuclear (Nuc.) and cytoplasmic (Cyt.) proteins (20 μg) were extracted for immunoblot analysis of PPARγ. Differentiated 3T3-L1 cell lysate (2 μg) was used as a positive control for the expression of PPARγ. Immunoblots shown are representative of n = 3. (**B-D**) VSMCs were transfected with scrambled (Scr.) or PPARγ siRNA followed by

maintenance in culture for 48 hr. Subsequently, VSMCs were pretreated with PIO (30 μM, 30 min) or vehicle control followed by exposure to PDGF (30 ng/ml, 48 hr) under serum-deprived conditions. The respective VSMC lysates were then subjected to immunoblot analysis using primary antibodies specific for PPARγ, CD36, pAMPK, pS6, pERK1/2 and cyclin D1. *$p < 0.05$ compared with scr. siRNA. Immunoblots shown are representative of n = 3. (**E**) Serum-deprived VSMCs were pretreated with PPARγ inhibitor (GW-9662; 10 μM, 30 min) followed by exposure to PIO (30 μM, 30 min) or vehicle control and subsequent exposure to PDGF (30 ng/ml, 48 hr). VSMC lysates were then subjected to immunoblot analysis for pAMPK, pS6, pERK1/2 and cyclin D1. Immunoblots shown are representative of n = 3.

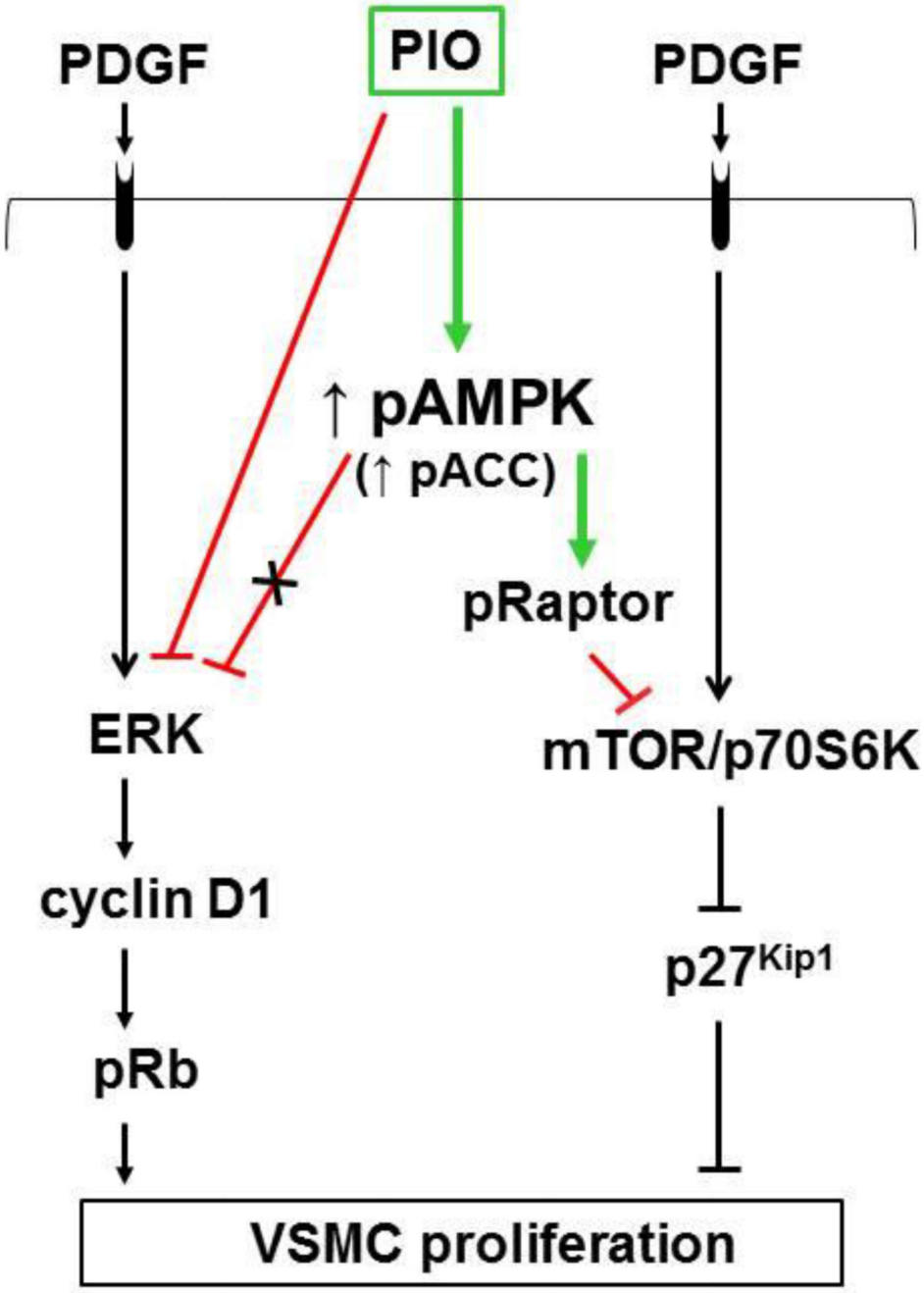

Fig. 8.

PIO inhibits PDGF-induced VSMC proliferation *via* AMPK-dependent and AMPK-independent mechanisms. PIO activates AMPK to promote raptor phosphorylation, thereby inhibiting PDGF-induced mTOR/p70S6 kinase signaling to facilitate $p27^{kip1}$ accumulation. In addition, PIO inhibition of ERK1/2 phosphorylation (that occurs independent of AMPK or PPARγ) results in the suppression of cyclin D1 expression and Rb phosphorylation.